Earthquake disaster database system in assessment and prediction of seismic hazard

PALLAVI[1], SANDEEP JOSHI[1,*], RANJIT DAS[2] and AMIT KUMAR BAIRWA[1]

[1]Manipal University Jaipur, Jaipur, Rajasthan, India
[2]Universidad Catolica Del Norte, Antofagasta, Chile
e-mail: sjoshinew@yahoo.com

Abstract. A homogeneous earthquake database is required to research earthquake occurrence patterns throughout time and space, as well as for a variety of technical applications such as seismic hazard assessment, peak ground acceleration computation, and long-term seismic strain rate estimation. Naturally, its seismic network and earthquake database have evolved in tandem with advances in seismology research. Magnitude is one of the most essential factors in determining the size of an earthquake, notably in seismic hazard assessment research. A rigorous and critical examination of these studies was created to compare various interpretations of existing earthquake data in terms of seismic characteristics (date, location, and size) and to determine the most trustworthy interpretation for each tremor. In terms of moment magnitude, the earthquake catalog is homogenized. The catalog compilation technique, the elimination of redundant events, the consolidation of magnitude scales, and the declustering process are used to remove dependent events, and its completeness analysis is well explained. Several magnitude-conversion method relationships, corresponding to known locals and regionals, have been constructed to offer uniform estimates of the moment magnitude for the whole collection.

Keywords. Seismic catalogue; magnitudes; seismic monitoring; seismicity; seismic source zone.

1. Introduction

Earthquake catalogs are a valuable seismological tool for resolving difficulties regarding earthquake location, antecedents, and source factors [1]. Catalogs are required to determine where, when, and how a fault bursts, in addition to earthquake precursors and seismic hazard analyses based on field data and theory. The definition of an earthquake is the shaking of the ground [2]. This is a completely natural occurrence. The earthquakes that make headlines are generally the most powerful. It is initiated by an energy discharge, which causes the waves to propagate in both directions. Seismic waves are the vibrations produced by earthquakes as they travel through the Earth and are recorded by seismographs [3, 4]. The hypocentre is the site of the earthquake under the surface of the earth, whereas the epicenter is directly above it on the surface of the earth. The Richter scale (Earthquake Scale) is employed to determine the magnitude of an earthquake. It is obtained from seismograms and explains the dependence of waveform amplitude on epicentral distance. Focal depth is an essential factor in determining the destructive potential of an earthquake. The majority of destructive earthquakes have focal depths of less than 70 kilometers. The epicentral

distance is the distance between the epicenter and any area of interest. The earthquake's magnitude is a numerical measurement of its size. These numerical magnitude scales have no upper or lower limits; the magnitude of a very tiny earthquake might be 0 or even negative [5].

Foreshocks are earthquakes that occur before the mainshock, which is the earthquake with the largest magnitude in a sequence of earthquakes. When compared to regular seismic activity, foreshock activity frequently exhibits substantial changes, such as a lower b-value and migration and acceleration before the mainshock [6]. Earthquake catalogs are the most important sources of data for building a seismic database to use in assessing seismic hazards. In general, earthquake magnitudes are reported on some magnitude scales, and it is believed that by translating many magnitude scales into a single one, a unified catalog would be generated [7].

Quarry explosions, for example, regularly contaminate earthquake records. It is crucial to distinguish these quarry explosion events from earthquakes to conduct legitimate seismicity and risk studies [8]. Earthquakes of smaller sizes were translated using empirical global equations, which were constructed and tested. With the use of a procedure, it is claimed that different magnitudes can be turned into moment magnitudes. In general, the magnitude categories in regional seismicity inventories vary, but analyzing a

complete and homogeneous earthquake inventory is required to determine the distribution of earthquakes in a region as a function of geography, time, and magnitude [9]. This worldwide library was also intended to serve as a reference for individuals constructing regional seismicity databases that comprise occurrences of considerably lower magnitudes. This ensures that the catalogs created by other teams for other areas have equivalent earthquake locations and magnitude information, particularly in border regions. Repeated earthquakes can help us understand earthquake-generating mechanisms, monitor local structural changes, and test earthquake forecasting. Recurrent earthquake analysis has shown regional distribution and temporal variations in their underlying mechanisms [10]. Table 1 shows different types of magnitude.

The main contribution of this paper is as follows:

- This document gives a list of earthquakes that have occurred in various places, as well as their characteristics.
- Global earthquake catalog is taken into consideration to display numerous variations of the earthquake.
- Different types of magnitude scales are also investigated.
- Finally, some potential future directions are examined.

The following sections of the paper are grouped as follows: Section 2 contains earthquake catalogs for several locations, including Turkey, Europe, Africa, Asia, Greece, and India, and, finally, a global earthquake catalog. Section 3 highlights the gaps that exist in the existing literature. Section 4. demonstrates the future trajectory of the paper. Finally, in Section 5 we conclude this article.

2. Literature Review

For the research region, the construction of a current and updated homogeneous earthquake catalog is required as part of a regular seismic hazard assessment process. To map seismic risks, it is necessary to have a comprehensive database of recent earthquakes, complete with particular epicenters and homogenized magnitudes, which can be accessed online. The epicenters, in particular, are based on local data, whereas the magnitudes are based on teleseismic readings, the majority of which are sourced from world-wide online cataloging services. In this project, the major purpose is to develop a standardized earthquake library that can be utilized in the analysis of seismic risks in many nations. The magnitudes are of several sorts, but only M_S, m_b, M_L, and M_W are examined in this case. Different country catalogs are discussed below.

2.1 *Turkey Catalog*

There are various earthquake catalogs for Turkey available, albeit most of them are just compilations of source data from other publications, with no recalculations performed. A total of 2700 earthquakes(within latitudes $35.5°$ N to $42.5°$ N and longitudes $25.5°$ E to $45.O°$ E) have been recorded in the database, with 450 of them having a magnitude greater than 5.0 in our database. This is seen in figure 1 which depicts the distribution of energy release Although the objective of data processing has been to establish consistency, the fact that the data is readily available puts a limit on our ability to achieve this goal. According to the following, we sought to assess the completeness of our collection in several different methods, as outlined below.

Table 1. Different types of magnitude.

| Sr.No.	Magnitude	Symbol	Characteristics
1	Local Magnitude	M_L	Commonly referred as Ritcher Magnitude.
			1935 for Southern California
			For high frequency magnitude only less than $7.3 \leq M_L \leq 7$.
2	Body Wave Magnitude	m_b	It is composed of P-waves that come first and, as a result of saturation, it is not able to represent correctly.
			Less than 7.
3	Surface Wave Magnitude	M_s	It travels along the Earth's surface and on Love waves.
			It measured the amplitude of surface wave for a period "of about 20 seconds".
			Up to 8.7 magnitudes.
			Above this again saturation takes place.
4	Moment Magnitude	M_w	1977-Kanamori.
			For South California, Not for Global.
			Not good for fewer magnitude earthquakes i.e., below 7.5.
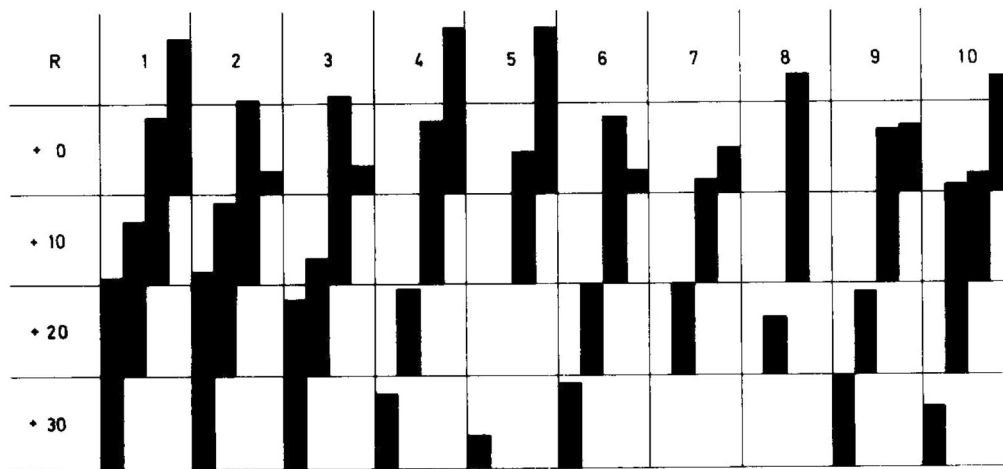
Figure 1. Seismic M 2 5.0 Logarithmic energy summations of earthquakes by area from 1913 to 1970 [11].

1. Three intervals have been analyzed in terms of frequency-magnitude relationships (N denoted half-unit intervals of M, which were thereafter decreased to low-year intervals;)

$$1918 - 1930 : logN = (5.11 \pm 0.07) - (0.68 \pm 0.01)M$$
$$1946 - 1955 : logN = (5.41 \pm 0.05) - (0.73 \pm 0.01)M$$
$$1964 - 1970 : logN = (6.00 \pm 0.01) - (0.78 \pm 0.02)M$$

As we can see from these three relationships, throughout time, not only the level but also the slopes have risen, a reflection of the more plentiful material that has been accumulated. No doubt, some of this may be attributed to advances in seismograph networks, but it might be attributable to genuine changes in Turkish seismicity as well. Although it is not particularly effective, graphing the released energy E vs time is another way to evaluate the completeness of data. E in ergs may be determined by multiplying the following by:

$$logE = 12.24 + 1.44M$$

summarised and displayed in a cumulative graphic each year.

On the other hand, the well-known 1.2-magnitude gap between a large earthquake and its greatest aftershock may be used as a test of completeness. As a result of averaging twenty earthquakes with M $\geq$ 7.0, we discover that this difference is higher(1.7) as a result of local influences [11].

Over the past 40 years, Turkey has been the site of fewer than 30 earthquakes with magnitudes of 6.0 or more. In the direction of Anatolia, smaller events (M $\geq$ 4.0) tend to concentrate in the west and east, as seen in figure 2. As seen in figure 2, the North Anatolian Fault System is experiencing just a moderate amount of activity. A catastrophic earthquake can occur, and between 1939 and 1957, there were six large incidents (M $\geq$ 6.5) occurred. To put it another way, current seismological observations in Turkey are insufficient to comprehend fault system behavior, according to this definition. Only 35 incidents happened before the birth of Christ, with seven of them taking place on the island of Crete between 2100 and 1400 B.C. Anatolia does not have any recorded incidents before 600 B.C. The focal mechanism characteristics of 108 devastating earthquakes, as well as historical earthquake data, have been gathered and analyzed. The data sets supplied here [12] should be used to help and enhance earthquake research in the future.

Many of the catalogs or statistics available for earthquakes in Turkey and the surrounding area have specific restrictions that must be met to make a risk assessment. A subproject of the Seismotectonic Map of Turkey Project has been created to produce a new inventory in response to the demands. In determining the source fault of the big earthquakes that triggered surface rupture, there is no room for doubt. One of the most dependable characteristics to use in determining the historical earthquake epicenter is a surface breach. This characteristic is used to link the location of a major earthquake that caused a surface rupture during the cataloging period with the location of the large earthquake. When it comes to earthquakes, the positions of the 1944 Gerede earthquake of M_w 7.4 given by different catalogs are considerably afield from those of the surface rupture caused by the strike-slip mechanism. The reference prosed close to the surface breach has been chosen as the epicenter of the 1944 event because of its proximity to the surface rupture figure 3. From 1900 to 2012, the new parametric collection covers 12,674 occurrences in Turkey and its neighboring areas. 203 occurrences with M $\geq$ 6.0 are presented in a way that will be of interest to earth scientists. Following significant active structures in Turkey and its surroundings, the epicentral sites are distributed [13].
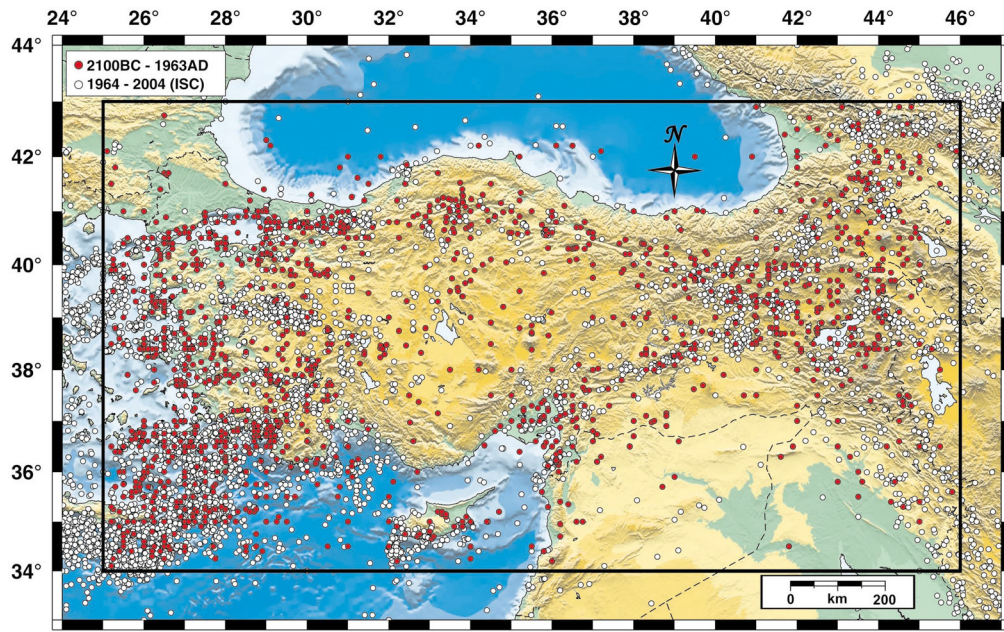
Figure 2. Turkey's seismicity map In the database, red circles reflect previous earthquakes. Active quakes are shown by white circles (M $\geq$ 4.0; ISC, 2001). There is a thick line that delimits the border of the historical earthquake data set [12].
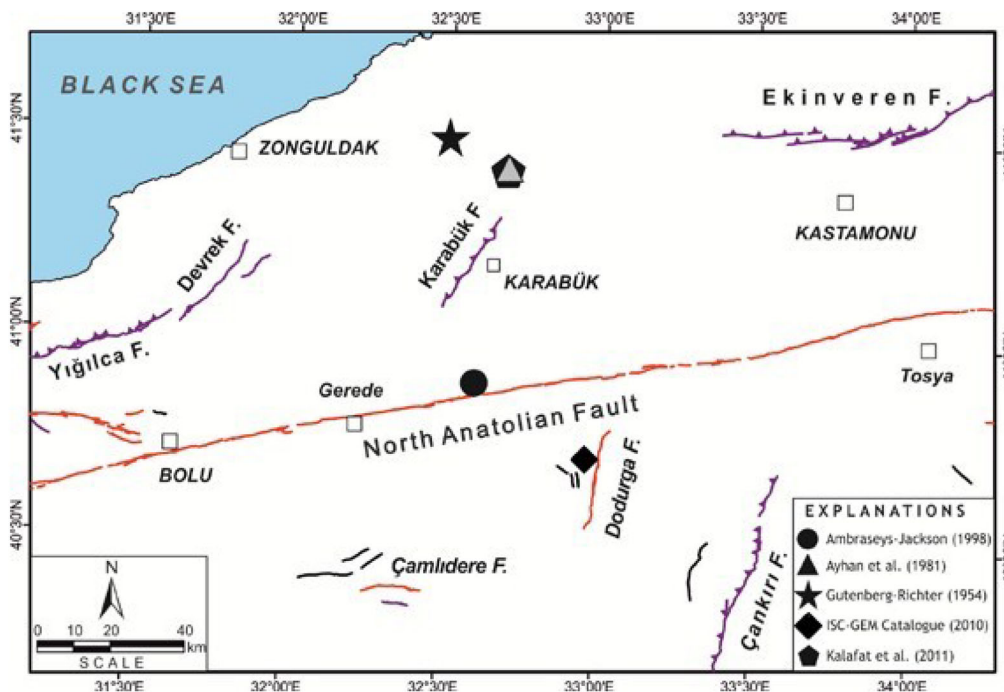

Figure 3. Variations in epicenter sites for the $M_w \geq 7.4$ Gerede earthquake of 1944, as stated by several catalogues [13].

During this investigation, more accurate and consistent input was retrieved from the integrated database, resulting in a library of 12,674 occurrences covering 1900. This was also true for the enhanced earthquake catalog, in which magnitude and depth characteristics were not reevaluated instead the most accurate values were chosen directly from the collected sources, according to previously determined criteria. There have been 203 and 1468 instances in M $\geq$ 6.0 and 5.0 $\leq$ M 6.0, respectively. It is completely over M_W 4.3 in its homogenized version. Once fore- and aftershock events have been removed, the catalog consists of 6573 occurrences. It turns out that foreshocks and

aftershocks account for half of the improved repertoire, according to the results of the Dec. Many foreshock and aftershock occurrences have happened in recent decades, even though they are not mentioned in the text. The finding is in line with the results of the completeness tests, which suggest that there were no small-scale events occurring up [14].

For seismological research, seismic hazard analysis, and the creation of attenuation relationships, empirical magnitude conversion relationships are significant factors. A freshly created earthquake library was used to derive new empirical magnitude conversion formulae for the translation from m_b to M_w, M_L to M_d, and M_S to M_w. For the new associations to be successful, they must make use of as many data points as possible, compared to the existing literature. The endeavor to update Turkey's seismic hazard map is funded by the AFAD National Earthquake Research Program, which has produced new empirical equations. We tried to construct conversion relations from the chosen magnitude categories (such as M_S, m_b, M_L, and M_d) to the moment magnitude in this work (M_W). Orthogonal Regression's(OR) residual scatters for conversions from M_S to M_W show almost little bias for both full data and $M_S \geq 4.0$. As a result, OR was judged to be the best technique to convert M_S to M_W. ISC M_S and M_W from HRVD GCMT, on the other hand, showed a greater physical relationship. This is the projected result when both magnitudes are measured over a long period. With $M_W \geq 5.8$ in particular, the M_S scales fit well. There was a significant slope in the linear trend between conservative and non-conservative values in the residual graph for the conversions m_b, M_L, and M_d to M_W performed by OR, in contrast to conservative values. This is why the OR technique was not initially accepted as a method of converting the magnitude to M_W. m_b, M_L, and M_d to M_W were converted using the OLS technique, and the residual graph trend line showed no significant slope [15].

Seismic clusters arise as a result of earthquakes that generate more earthquakes and form clusters in space and time. In seismic research, particularly in probabilistic seismic hazard assessment, declustering is regarded as a necessity, to decrease bias and disassociate major shocks and triggered events from mainshocks. The purpose of this project is to measure how different clustering approaches affect the estimation of seismic hazards. As a consequence, the newly created Turkish earthquake catalog was declustered using three declustering methods. In all, six declustered catalogs were created: two catalogs for each approach (one with default input values, and one with free input parameters). These earthquake clusters were investigated in terms of how earthquake sequences are distributed spatially and temporally. Stakeholders in Istanbul's seismic hazard assessment have carried out a sensitivity analysis of the key phases involved in the process. Both the 475-year and 2475-year return periods showed more strong impacts for Peak Ground Acceleration (PGA) and 5 percent damped

computed horizontal spectral acceleration(Sa) at T = 0.2 s than for percent 5 damped Sa at T = 1.0 s. This study demonstrates that utilizing different declustering methods can result in extremely different acceleration results, in this situation, PGA and Sa at 0.2 s can be increased by up to 20%. The choice of a clustering approach is critical to calculating seismic hazard levels and assessing seismic risk, both of which are related to the estimation of earthquake loss and decision-making processes based on these findings [16].

The Marmara section of the North Anatolian Fault Zone (NAFZ) in Istanbul's near vicinity is expected to create earthquakes in the following few decades, from magnitude M up to 7.4. Our catalog has a regional completeness moment magnitude of $M_c = 2.1$ during the last decade (2006-2016). Because of this, the Marmara Section, or the northern NAFZ strand of the fault, is the most seismically active fault strand. For the Sea of Marmara, we provide a revised hypo-center database, including 6,812 earthquake sites reported over 10.5 years between the years 2006 to 2016. 4,407 earthquake sites can be pinpointed using relative relocation. To calculate the magnitudes of these earthquakes, the moment magnitudes of 5,353 earthquakes and the focal mechanisms of 140 earthquakes are calculated. Based on our findings, we reviewed seismic records from a variety of permanent networks, including the Disaster and Emergency Management Presidency of Turkey (AFAD) and the Kandilli Observatory and Earthquake Research Institute (KOERI), which operate the region's two largest seismological networks. Our absolute (and relatively shifting) earthquake hypocenters are responsible for over one-third of the 12,000 earthquakes reported by national seismological services and other researchers. Because only a small fraction of the network captured them, the number of earthquakes that can be precisely located has decreased significantly. Throughout an active seismotectonic age that may result in a big M $\geq$ 7 quakes, the ultimate relative movement of hypocenters gives continuous long-term observations of regional seismic activity along with the North Anatolian Fault Zone's Marmara Section, a risk to Istanbul's infrastructure [17].

As part of the project, a new earthquake catalog has been created covering the period 1900-2017 for Turkey and neighboring areas (32°–47° N, 20°–52° E). The ISC Bulletin of Seismological Parameters is the source of earthquake parameters, which will be fully updated in 2019. New conversion equations between moment magnitude and several scales (m_d, M_L, m_b, M_s, and M) that use the General Orthogonal Regression technique to produce a homogenous collection of seismic hazard data are available. The magnitude of completeness in Turkey and Greece is 3.5-4.0 M_w and 2.5-4.0 M_w, respectively. The number of events recorded with local magnitude (M_L) is 443,939 (64 percent of the total) and has the highest rate of 130 compared to the other magnitude categories (1964-2017) (figure 4). Approximately 700,000 occurrences are gathered in the
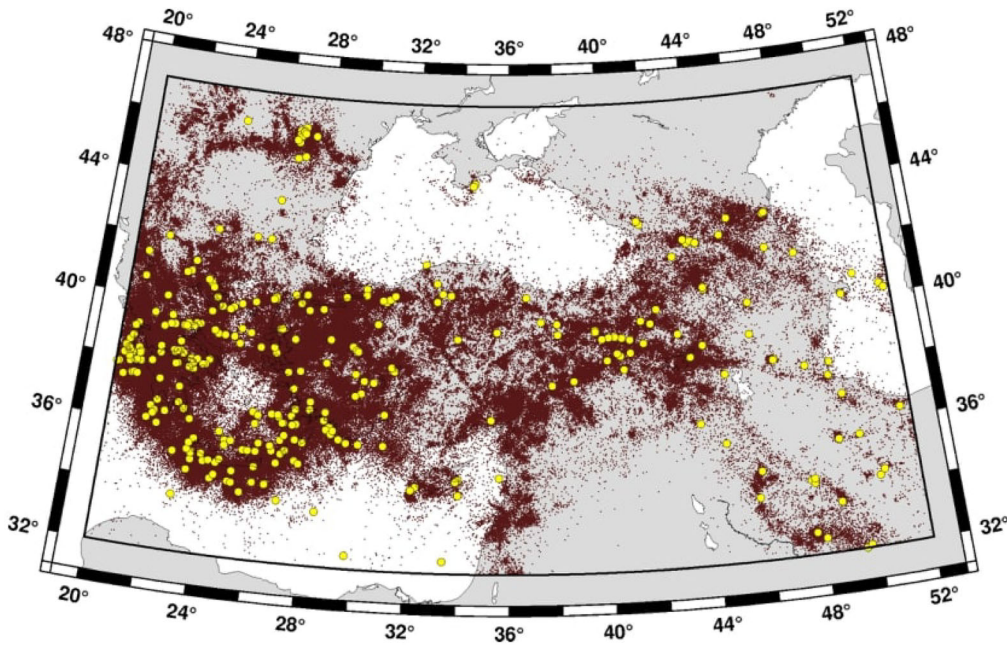
Figure 4. The catalog region (solid boundary) and the earthquake in the catalog took place between 1900 and 2017. (dots). Yellow circles represent occurrences with magnitudes greater than 6.0 [18].

research region. For all occurrences, the magnitude of the corresponding moment (M_w*), which is a required seismic hazard parameter assessment, is computed. As a result, new conversion equations for m_d, M_L, m_b, M_s, and M are identified in the general orthogonal regression technique that employs the well-refined magnitude pairing 340, which is useful when the two variables have various degrees of uncertainty. The entire catalog is comprehensive down to $M_c = 2.9$, based on M_w* values. $M_c = 3.0 - 3.2$ in Turkey, according to the variation in geographic completeness. Seismologists and earthquake engineers can simply recalculate the values of $M_w *$ and divide the catalog using different parameters for seismic hazards analysis. In addition to M_w*, as in prior research, the final dataset comprises the observed magnitudes' average, standard deviation, and median. The general orthogonal regression is used to evaluate the associations between the refined magnitude pairs (GOR). The general orthogonal regression is used to evaluate the associations between the refined magnitude pairs (GOR). However, GOR is incorrectly used in seismic literature because it does not encounter equation errors. The slope values of the GOR line (m) and intercept (c) values in the form $y = mx + c$ are provided by the

$$m = \frac{S_B^2 - \eta S_A^2 + \sqrt{(S_B^2 - \eta S_A^2) + 4\eta S_{A_B}^2}}{2S_{A_B}} \quad (1)$$

$$c = \bar{B} - a\bar{A}. \quad (2)$$

where S_A^2, S_B^2 and $S_{A_B}^2$ denote the A (independent variable), B (dependent variable), and A and B covariance. The

variable's average values are A and B. η is the variable's error variance ratio [18].

Table 2 shows the comparative analysis of the Turkey Catalog. The comparison is done between different magnitudes used in the catalog, the year of the catalog, and the latitude and longitude of the area where the earthquake occurred.

2.2 *Europe Catalog*

The article offers the findings of a review of the Croatian earthquake inventory for the years 1908-1992. Based on a temporal study of the best probability estimate of the b-value in the frequency-magnitude relation, the catalog is judged to be complete for occurrences with $M \geq 4.0$ within the analyzed time. After the midcentury mark, the magnitude completeness threshold falls to 3.8 and then to roughly 3.6 in the last three decades. It is shown that the change in b-value with time is highly related to seismic activity and that there appears to be a scarcity of seismic energy release during the $M = 6.0$-6.5 earthquake. For all instrumentally localized earthquakes, this database's micro-seismic component already exists in digital form. Its macroseismic component will be developed as a result of a newly begun initiative to digitize all current isoseismal maps. The entire catalog (including instances with $M_L \geq 3.5$) is available in magnetic media for scientific purposes only on request of the original author [19].

For regions "44° N-72° N, 25° W-32° E", from 1300-1993, the catalog contains tectonic events from the databank. $M_w = 3.50$ is the lowest magnitude level for

Table 2. Comparative study of Turkey Catalog

Author	Title	Magnitude	Year	Lat/Long
Esen Alsan et al. [11]	"An Earthquake Catalog for Turkey for the Interval 1913-1970"	M_s and m_b	1913–1970	35.5° to 42.5° N / 25.5° to 45.0° E
Onur Tan et al. [12]	"The Earthquake Catalogues for Turkey"	M_w	2100 B.C. 1930 A.D.	34° to 43° N / 25° to 46° E
F. Tabu Kadirioglu et al. [13]	"An Improved Earthquake Catalog (M ≥ 4.0) For Turkey And Near Surrounding (1900–2012)"	M_w, M_s, m_b, M_L, and M_D	1900–2012	32° to 45° N / 23° to 48° E
F. Tabu Kadirioglu et al. [15]	"An improved earthquake catalog (M ≥ 4.0) for Turkey and its vicinity (1900–2012)"	M_w, M_s, m_b, M_L and M_D	1900–2012	32° to 45° N / 23° to 48° E
T. Eroglu Azak et al. [16]	"Effects of seismic declustering on seismic hazard assessment: a sensitivity study using the Turkish earthquake catalog"	M_w	1900–2012	N.A.
Christopher Wollina et al. [17]	"A unified earthquake catalog for the Sea of Marmara Region, Turkey, based on automated phase picking and travel-time inversion: seismotectonic implications"	M_W	2006–2016	40°45' N / 27°30' to 29° E
Onur Tan [18]	"A Homogeneous Earthquake Catalogue for Turkey and Surrounding Region"	M_w, M_s, m_b, M_L and M_D	1900–2017	32° to 47° N / 20° to 52° E

Catalogue entries. Depending on the priority system, M_w is determined by using one of the magnitude categories or macroseismic data provided by the chosen entry. Each Catalogue item includes the genesis time, location, M_w magnitude, and reference. The epicentral intensity, I_0, is also given by the source. The magnitude concept M_L is by far the most prevalent in the Databank. It is the only magnitude assigned to many earthquakes. The tightly bound relationship

$$M_w = 0.67(\pm 0.11) + 0.56(\pm 0.08)M_L + 0.046(\pm 0.013)M_L^2 \tag{3}$$

The chi-square maximum likelihood regression model used in this paper is based on authentic seismic moment data from 164 earthquakes in Central Europe (figure 5). The two deadly Vrançea earthquakes of the previous century, in 1940 (M_w = 7.7) and 1977 (M_w = 7.4), were significantly more numerous than the most severe incidents in the entire Central and Northern European region recorded dating back to 1300 [20].

Depending on the scale and location of an event, three types of research were carried out: historical, macroseismic, and seismological. All accessible historical data for earthquakes of intensity 6 or greater in the last 1000 years was gathered, and macroseismic fields were created. After that, the uncertainties in the source parameters (epicenter, hypocentral depth class, epicentral intensity, maximum intensity, and macroseismic magnitude) were estimated. 177 of these occurrences were classified as having intensity 6 in the revised inventory and, therefore, caused damage. Due to various calendar designs, misprints, or misunderstood compilations, approximately 260 events may be identified as bogus events or multiple entries for the same
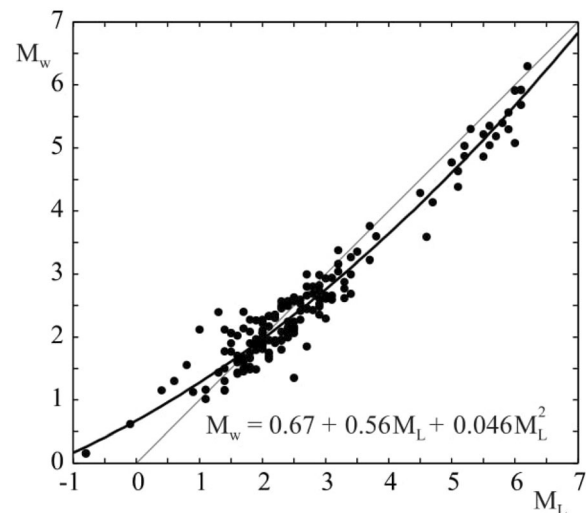

Figure 5. For Central Europe, input data and the M_w vs. M_L chi-square maximum likelihood regression curve, eq. 3. For comparison, the $M_w = M_L$ line is drawn [20].

occurrence. For all occurrences, the catalog gives a consistent estimate of the magnitude of the moment M_w. ECOS (Earthquake Catalog of Switzerland) is a new comprehensive earthquake catalog for Switzerland and adjacent regions that cover all seismogenic locations that provide a substantial seismic risk to Switzerland. The revised Macro Seismic Earthquake Catalog of Switzerland (MECOS-02) is at the heart of ECOS, it also offers a complete, homogeneous database of historical and macroseismic data created by gathering and analyzing sources and historical data compilers, in addition to combining all available macroseismic data and earthquake investigations. ECOS distinguishes itself by consistently evaluating the parameters of the earthquake, including the standard magnitude M_w for all the occurrences and an assessment of the error boundaries for all the source parameters [21].

The chi-square approach can take into account individual entry mistakes, but it can also be used when faults are not precisely known and only lesser quantitative limitations can be imposed. The results of three different types of regression models are depicted: (1) a linear relationship between M_S and m_b for North Atlantic Ocean occurrences; (2) a quadratic relationship between M_w and M_L for central European events; and (3) for some places in central and northern Europe, there are linear relationships between M_L and I_0, having a logarithmic relationship between the focal depth. The development of earthquake catalogs frequently necessitates the use of empirical relationships for the translation of macro conversions of seismic data to magnitude and magnitude conversions between different magnitude categories. For magnitude correlations with uncertainty in all input variables, a generalized chi-square regression technique is used. Individual error distributions for each input data might be considered. In most circumstances, a chi-square technique can retain the empirical relationship symmetry, assuring path-independent magnitude determination in a conversion hierarchy. An orthogonal regression strategy, which is generally recommended in such cases, is only relevant if the regression model is linear and the unknown input errors are consistent across all data sets [22].

Due to considerably increased seismicity in the new region, the threshold for occurrences south of latitude 44° N has been set at $M_w \geq 4.0$, retaining the lower barrier in the northern catalog part. The homogeneity of the new Euro-Mediterranean Earthquake Catalogue(EMEC) for M_w was investigated and improved when possible. EMEC has records for around 45,000 earthquakes. In contrast to [23], the focal depths of crustal tectonic earthquakes are rather shallow, frequently inadequately defined, and are not recognized, since they are occasionally published in catalogs with magnitudes M_L. Such combinations of magnitude and depth would result in intensity levels that would not have been detected otherwise. As a result, only depths of 3 km or greater for M_w = 3.5 to 3.9 events, 5 km or greater for M_w = 4.0 to 4.4 events, and 7 km or greater for M_w geq 4.5 events are included in the database and used in calculations where a depth term is used to calculate M_w from the intensity are included. Figure 6, which is limited to earthquakes of $M_w \geq 6.0$, shows an even stronger relationship
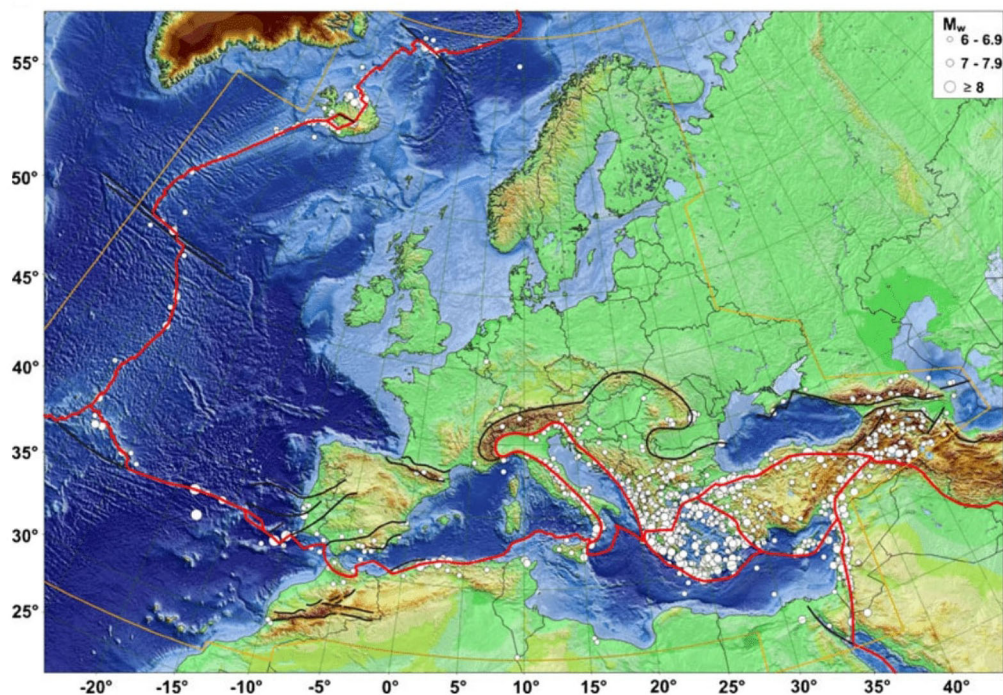

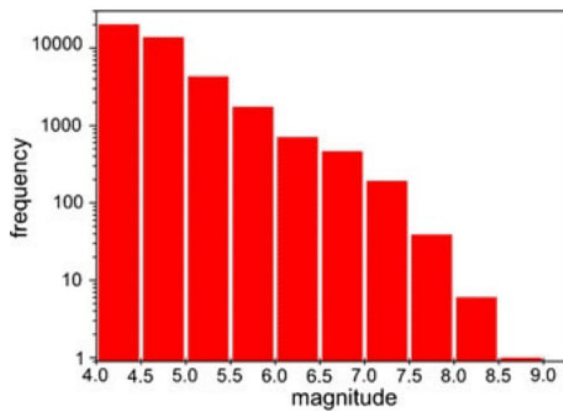**Figure 6.** Events involving $M_w \geq 6.0$ [24].

Figure 7. The frequency of earthquakes in half-magnitude classes from the EMEC catalogue [24].

of seismicity with active tectonic characteristics. Except for a few examples, the Alpide belt and other plate boundaries are related to seismicity M_w geq 6.0. This graph also shows that most of the $M_w \geq 7.0$ occurrences are associated with plate boundaries, specifically the subduction zone of the Aegean. Figure 7 depicts a histogram of the number of occurrences of various magnitude classes in EMEC. In recent years, the availability of earthquake catalogs or data files have decreased rather than increased [24].

In 1991, Iceland established a new seismic monitoring network known as SIL, which featured computerized seismic technology and autonomous operations. The gadget is outfitted with software that warns users of the location and magnitude of earthquakes 1-2 minutes after they occur. In Iceland, we investigated the implications of utilizing the network criteria technique to filter the SIL catalog. Although the network is not as dense as it is in many other
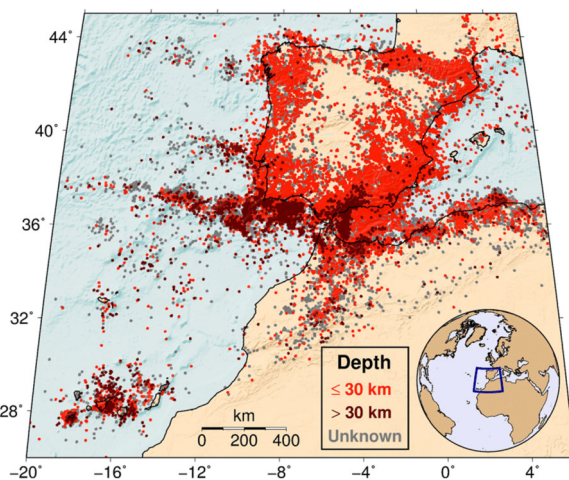

Figure 8. Epicenters from the beginning of time until the end of 2013 in the Spanish National Earthquake Catalog, divided by hypocentral depth. Depth is considered unknown if it is absent (as in the case of occurrences discovered only based on intensity data) or fixed (not computed as a distinct parameter) [24].

parts of the world, we found the filter to be extremely severe in this area, where the emphasis is on identifying microseismicity: practically because there were insufficient arrival time selections, all microearthquakes were filtered out. Based on the multivariate distribution of hypocentral uncertainty, we offer an alternative filter. We discovered and eliminated 502 such occurrences (*sim* 0.4% of the earthquakes in the filtered collection). We discovered and corrected many errors in the SIL catalog's estimation of local magnitude and what is known as local moment magnitude. The scale of great events, in particular, is typically overestimated, and the importance of small events that occur after major events is often exaggerated [25].

This report describes the history, precision, and completeness of the Spanish National Geographic Institute's earthquake inventory. This database contains almost 100,000 earthquakes that occurred in an area that includes Spain, Portugal, Morocco, Andorra, and portions of France and Algeria. Earthquakes are more commonly observed at night and on weekends, owing to decreased artificial noise. Figure 8 shows the epicenters and geographic breadth of the catalog ($26° N$ to $45° N$, $20° W$ to $6° E$). The database has information on more than 100,000 occurrences dating from 880 B.C. to 2016, with the bulk occurring in recent decades and an annual record of 17,000 in 2011. The catalog contains a temporal and geographical combination of magnitude scales that are not equal. Such variability is known to impact, for example, other catalogs, seismicity rates, and b-values should be considered. thoroughly investigated before any statistical research. Improvements in earthquake detection have enabled the region to record a growing number of earthquakes per unit period, indicating a gradual reduction in the magnitude of completeness, M_c [26].

In 1991, Iceland built a digital seismic monitoring network that included a digital seismic system and self-contained operations. We explore its national performance for the first time after 20 years of operation by investigating the Spatio-temporal fluctuations in the level of completeness. We find that the magnitude of completeness M_c for the entire active rift zone of the north-south is in the range of 0.5 to 1.0, underlining the ability of the Icelandic network to detect tiny earthquakes. This value M_c was maintained until 2002 because, in addition to the Hengill seismic swarm, a seismic series began in the South Iceland Seismic Zone (SISZ) region in June 2000, as a result of the occurrence of two big earthquakes (moment magnitude greater than 6.0). At the end of this period of strong seismicity, the value of M_c had risen to 0.9 (Figure 9).

In all tectonically active regions, the total range fluctuated between 0.2 and 0.5 in the transform zone and between 0.5 and 1.5 in volcanic zones, from the Tjörnes Fracture Zone (TFZ) to Northern Volcanic Zone (NVZ) to Reykjanes Peninsula (RP). In areas with high station coverage, the Bayesian magnitude of completeness (BMC) standard deviations might be as low as 0.1. Moving farther away from these points, where there are fewer stations, increases
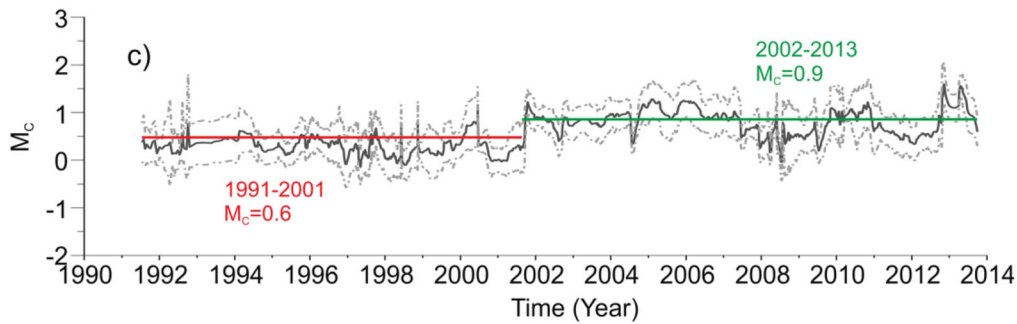
Figure 9. The dotted lines represent the standard deviation of the magnitude of completeness over time. The red and green lines represent the average values M_c from 1991 to 2001 and 2002 to 2013 [27].

both M_c and the standard deviation. Approaches such as BMC can be used to optimize the geometry of a seismic network in terms of the number and density of seismic stations during network construction, as well as in existing networks to improve the quality of completeness magnitude estimates [27].

This study describes the technique used to create a parametric earthquake library for metropolitan France. Both instrumental and historical eras are covered using moment magnitude (Mw) as the reference magnitude scale. The French seismic catalog (FCAT-17) collection is made up of the SIGMA (Seismic Ground Motion Assessment; EDF-CEA-AREVAENEL) historical parametric catalog (magnitude range: 3.5 to 7.0), which spans the years AD 463 to 1965, and the SiHex instrumental inventory, which spans the years 1965 to 2009. No magnitude conversion was utilized to determine M_w in the case of big instrumental occurrences ($M_w\ geq$ 3.4) and historical events. This helps to remove the uncertainty associated with the use of magnitude conversion relationships. In the SIGMA research on the historical era, a combined inversion of M and depth benefits 27 percent of the SIFRANCE occurrences. It is concerned with occurrences that have a pleasing macroseismic field with a consistent decrease in intensity with distance. Due to their poorly confined macroseismic field, to compute M_w, 73% of historical earthquakes require an a priori depth estimate. Because an incorrect inversion method might yield erroneous findings, any occurrence that provides unusual M_w and depth estimates for the geological and seismic environment of the defined region is extensively investigated. This is extended 40 kilometers beyond the French border to account for ambiguity in the position of the SISFRANCE epicenter and to restrict occurrences to those who have high confidence in their calculated magnitude and depth. Simultaneously, SiHex events are only supplied within France's borders plus a 20-kilometer buffer, because the SiHex initiative does not have an authoritative source of data acquired outside the exclusive economic zone at sea [28].

The goal of this research is to create the most comprehensive inventory of focal mechanisms for Romanian earthquakes that occurred between 1929 and 2000 in the Carpathian Orogen, Moesian and Moldavian Plateau, and Transylvanian Basin. From 1929 to the present, the collection comprises 250 crustal events and 416 intermediate-depth occurrences. Based on new catalog data and seismotectonic research, we propose a reconfiguration of the seismogenic zones located in the southern Carpathians toward the western side of Romania. We updated numerous sets of data, recalculated and modified certain parameters, and achieved a consensus to generate a near-final version consistent with more current and less ambiguous focal processes. Beginning in 1929, during the aforementioned period, there are 226 crustal events and 406 intermediate-depth occurrences on the list. The catalog of Romanian Earthquakes Focal Mechanisms(REFMC) library is being built as a robust database for a wide range of potential applications, including (1) Modeling the parameters of the primary stress field in Romania to correlate with the latest tectonic and geodynamic data; (2) Seismic Hazard Modeling Based on the Stress Field at the crustal and subcrustal levels; and (3) Contributing to a comprehensive geodynamic model of the Vrancea area capable of accommodating all geological/tectonic and geophysical/seismic observations [29].

To be compatible with the Global Centroid Moment Tensor project's M_w standard estimates, the magnitudes of all occurrences are equally revalued. Catalogs and online resources for the Italian region were merged, and all magnitudes were homogenized to *Mw* based on empirical links discovered using the chi-square regression technique, which correctly accounts for the uncertainties of both variables. The Homogenized Instrumental Seismic (HORUS) catalog is available for free download at hor-us.bo.ingv.it (last accessed July 2020). The Istituto Nazionale di Geofisica e Vulcanologia (INGV) Italian Seismological, Instrumental, and Parametric Database (ISIDe) from 2005 to the present (ISIDe Working Group, 2007) is available at http://webservices.ingv.it/. (Last accessed April 2020). We developed an automated system to create and update the Italian seismic database HORUS, with the magnitude transformed to be homogeneous with

the M_w estimated by the Global CMT project. Until 2012, the ability to average the converted M_w proxy from both M_L and M_D avoided this difficulty. We expect that INGV will opt to give M_D for all earthquakes in the future since, while less accurate than M_L, it provides extra information on earthquake size due to various measured factors. We check for potential flaws in the method by comparing the most recent version with the previous and sending an email if an unusually large number of differences are discovered.

Table 3 shows the comparative analysis of the Europe Catalog. The comparison is done between the different magnitudes used in the catalog, the year of the catalog, and the latitude and longitude of the area where the earthquake occurred.

2.3 *Africa Catalog*

The current project's purpose is to create and maintain a database of Egypt's instrumentally recorded earthquakes with consistent and homogenous source characteristics needed for seismic analysis and risk assessment. The observational data span the years 1900 to 2004 and a geographic range of 22° - 33.5° *N* and 25° - 36° *E*. The first (1900-1984) looks to be complete for $M_w \geq 4.5$, whereas the second (1985-2004) appears to be complete for $M_w \geq 3$. The data in that library include event locations, magnitudes, and macroseismic information for certain notable earthquakes; that occurred in the early instrumental period (1900- 1984). Helwan's local magnitude (M_L), seismic moment (M_o), moment magnitude (M_w), and duration magnitude (M_D) were the magnitudes covered in the second period (HLW). The number of occurrences climbed dramatically between 1998 and 2004. The number of incidents recorded in this short period is 9719. This is around 26.2 and 1.7 times higher than the first (1900 -1984) and second (1985-1997) epochs. This time contained Helwan's local magnitude ML, as well as the actual ISC's m_b and M_S and Helwan's local magnitude M_L. (IPRG). The coefficients of the two distinct log M_o-M_L(IPRG) relations are 1.0 and 1.35 in the two ranges of $1.7 \leq M_L \leq 3.4$ and 3.5 B M_L 6.0, respectively [31].

During the Jurassic era, the coastal boundary fault became tectonically active and is probably still active today. Tens of kilometers southwest of Accra, the two fault systems join and most of the seismic activity has been detected at this juncture. Damaged earthquakes in Ghana have been described in historical texts dating back to 1615. The two biggest catastrophic earthquakes that devastated Southern Ghana happened in 1862 (intensity IX) and 1939 (intensity IX) near the capital city of Accra (intensity VIII).

The seismometer stations are depicted on the map in Figure 10. A repeater station has been built in the eastern part of Amanokrom to enhance signal transmission from the outstations to the main observatory. The database's epicenter map reveals that the most seismically active places are in the country's southeast, where the Akwapim

fault zone and the coastal boundary fault intersect along Ghana's coast and the Akwapim Range. For building code applications, deterministic seismic hazard maps can now be constructed with unique hazard elements such as macroseismic intensity, maximum ground acceleration, or spectral acceleration [32].

This article presents an earthquake inventory for the Red Sea area with a unified moment magnitude (M_w). The value b was derived from all the data, and the 'a values for each source zone were gathered consecutively. The database may be used to produce a probabilistic assessment of the seismic threat in the Red Sea region. A seismotectonic model was attempted using geological, structural, and seismic data. For each zone, the seismicity and b-value parameters are calculated. The acquired unified M_w-based inventory is the first of its type in "the Red Sea Region" and serves as a first step toward assessing the region's seismic danger. The cataloging job is not complete; future research may reveal that this catalog can be improved and updated with the use of other databases. The axial rift between "the Red Sea" and "the Gulf of Aden", "the Red Sea beaches of Saudi Arabia and Yemen", and "the Afar triple junction of the Red Sea and the East African Rift System" has the highest frequency of earthquakes. Depth - Since 1915, known earthquakes have been reported, with the bulk of occurrences occurring between 1 and 30 kilometers under the earth's surface [33].

The Ethiopian Rift, which is part of the East African Rift system, cuts through the country's center, making it one of the world's most seismically active locations. The primary purpose of the study is to first consolidate and homogenize Ethiopia's earthquake database, after which "the Read Sea" and "Gulf of Aden regions" were turned into the Moment magnitude M_w scale utilizing completeness analysis in time and magnitudes. Second, we exhibit b values for different seismic zones and understand their implications for magma-induced seismicity at the locations. The current research area is restricted by latitude (4° *N* 20°) N and longitude (34° *N* 48°)*NE*, with a magnitude range of M_w (3.0-7.1) and a general coverage duration of 56 years (1960 to 2016). The mean a = 8.49 and the value b = 1.21 ± 0.04, the magnitude of completion (M_c) = 4.8 and the completion period from 2005 to 2014 are estimated for "the Afar rift" and "the Dabbahu magmatic section". The seismicity characteristics (average) for Northern Main Ethiopian Rift (NMER) are as follows: a = 5.77, b-value = 0.843, Completeness magnitude (M_c) of 3.2, and Completeness period of 3.2. (2001-2003). Central Main Ethiopian Rift (CMER) has a value of 4.33 and a b value of 0.826, a magnitude of completeness (M_c) of 3.1, and a completeness period from 2001 to 2003. Finally, the seismicity parameters (average) a = 6.9 and b-value = 1.03 for Southern Main Ethiopian Rift (SMER), as well as the magnitude of Completeness (M_c) = 5.1 and the completeness period 1960-2016, are computed. We discovered that b-values are used to map magma chamber movement,

Table 3. Comparative study of Europe Catalog.

| Author	Title	Magnitude	Year	Lat/Long
Marijan Herak et al. [19]	"Revision of the ' earthquake catalog and seismicity of Croatia, 1908-1992"	M_L	1908-1992	45° 10' N / 15°30' E
Gottfried Grünthal et al. [20]	" An M_w based earthquake catalog for central, northern and northwestern Europe using a hierarchy of magnitude conversions"	M_w	1300-1993	44° to 72° N / 25° to 32° E
D.Fah, D.Giardini et al. [21]	" earthquake Catalogue of Switzerland (ECOS) and the related macroseismic database"	M_w	1300-1970	45.3° to 47.9° N / 5.6° to 11.1° E
Dietrich Stromeyer et al. [22]	" Chi-square regression for seismic strength parameter relations, and their uncertainties, with applications to an M_w based earthquake catalog for central, northern and northwestern Europe"	M_w	N.A.	N.A.
Gottfried Grünthal et al. [24]	"The European-Mediterranean Earthquake Catalog (EMEC) for the last millennium"	M_w and M_0	1000-2006	40° N / 10° E
Francesco Panzera et al. [25]	"A Revised Earthquake Catalog for South Iceland"	M_w	1991-2013	63.75° to 64.15° N / -22.8° to -19.6° E
Alvaro Gonzalez [26]	"The Spanish National Earthquake Catalog: Evolution, precision, and completeness"	M_D and M_w	1900-2013	36° N / 10.8° E
Francesco Panzera et al. [27]	" Spatiotemporal evolution of the magnitude of completeness of the Icelandic earthquake catalog from 1991 to 2013"	M_L	1991-2013	63° to 67.5° N / -26° to -13° E
K.Manchuel et al. [28]	"The French seismic CATalogue (FCAT-17)"	M_w	1965-2009	43° N / 7.9° E
M. Radulian1 et al. [29]	" Revised catalog of earthquake mechanisms for the events occurred in Romania until the end of twentieth century: REFMC"	M_w, M_L, M_s, and M_D	1929-2000	44° to 50° N / 24° to 30° E
Barbara Lolli et al. [30]	" The Homogenized Instrumental Seismic Catalog (HORUS) of Italy from 1960 to Present"	M_w and M_D	1960-2005	N.A.
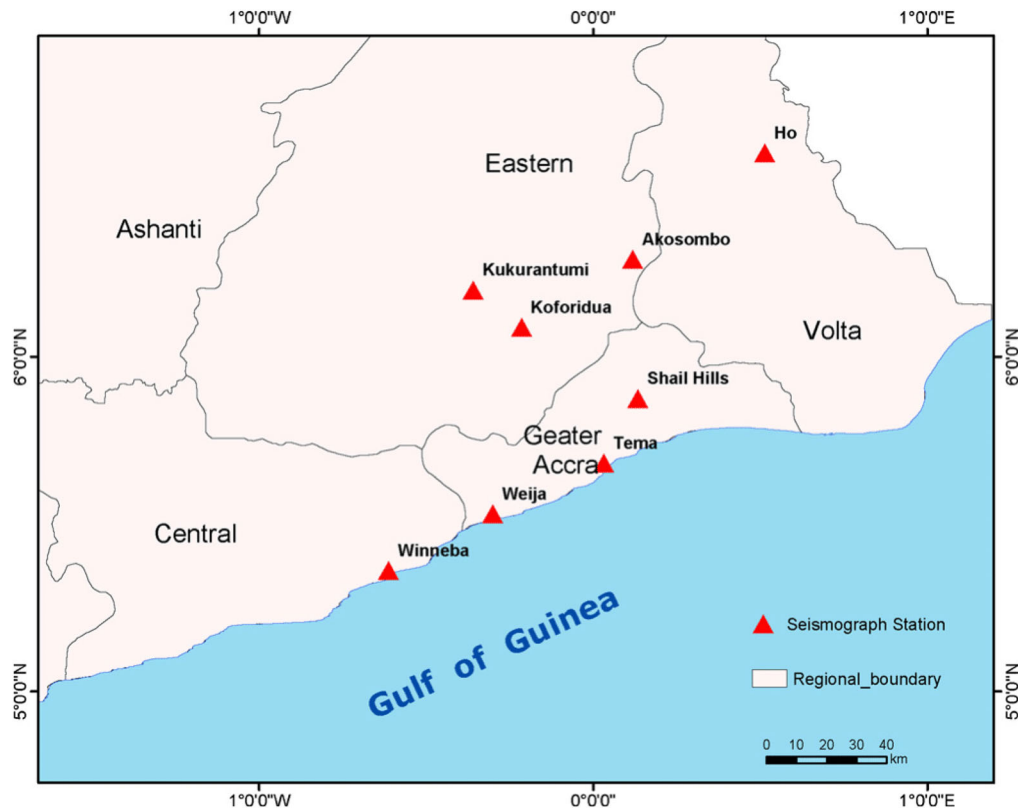
Figure 10. Seismograph sites in southern Ghana are depicted on a map [32].

which includes the charting of volcanic centers and magmatic segments. Furthermore, the values b can be used to map the lines and faults [34].

Table 4 shows the comparative analysis of the Africa Catalog. The comparison is made between different magnitudes used in the catalog, the year of the catalog, and the latitude and longitude of the area where the earthquake occurred.

2.4 *Asia Catalog*

The EEPAS model ("Every Earthquake a Precursor according to Scale") is an earthquake forecasting method that assumes the precursory scale increase (Ψ) phenomena occur at all stages of the seismogenic process. From 1965 through 2001, in the Japan region, a second test of the EEPAS model was carried out, firstly on earthquakes with magnitudes larger than 6.75. Over the learning period 1926-1964, the JMA catalog was fitted with a baseline model and the Gutenberg Richter b-value. When the EEPAS model was applied to data from Japan, it demonstrated the model's capacity to anticipate seismic activity in a seismic zone far more active than New Zealand and California, where it had previously been used. Without refining the settings, the superior performance of EEPAS over PPE in Japan demonstrates that the precursory scaling

relations are similar in New Zealand, California, and Japan. Nonetheless, the improved performance obtained by optimizing key EEPAS model parameters for Japan demonstrates that the magnitude scaling of precursors and large earthquakes differs between the two locales. More studies are needed to explain these disparities and determine the applicability of the model to other well-cataloged locations [35].

For Iraq, a probabilistic seismic hazard analysis (PSHA) was performed. The earthquake catalog used in this study covers an area between "latitude 29° - 38.5° N and longitude 39° - 50° E" and comprises over a thousand incidents spanning the years 1905 to 2000. According to the completeness research, the earthquake inventory is incomplete for all of Iraq and seismic source zones S1, S4, S5, and S8, with variations for the other seismic zones below $M_s = 4.8$. For all of Iraq, M_c was projected to be around $M_s = 4.0$, but S11 reveals that the lowest M_c for S4 is around $M_s = 3.5$ and the highest M_c is about $M_s = 4.2$. The seismic activity parameters (activity rate λ, b value, maximum regional magnitude *mmax*, and mean return period (R) with a particular lower magnitude $m_{min} \geq$ m and their likelihood of occurrence) have been computed for each of Iraq's 13 seismic source zones. Better estimates of the slope b following incompleteness treatment have been obtained in sources S7, S11, and S6, which tend to raise the slope b by

Table 4. Comparative study of Africa Catalog.

Author	Title	Magnitude	Year	Lat/Long
H. M. Hussein et al. [31]	"Integration and magnitude homogenization of the Egyptian earthquake catalog"	M_w	1900–2004	$22°$ to $33.5°$ N / $25°$ to $36°$ E
Paulina Amponsah et al. [32]	"Earthquake catalog of Ghana for the period 1615-2003 with special reference to the tectono-structural evolution of south-east Ghana & Earthquake catalog of Ghana for the period 1615-2003 with special reference to the tectono-structural evolution of South-East Ghana"	M_L and M_D	1615–2003	$5.10°$ to $5.57°$ N / $-1.30°$ to $-0.38°$ E
N. Babiker et al. [33]	"A unified M_w-based earthquake catalogue and seismic source zones for the Red Sea region"	M_w	2150 B.C.–2006 A.D.	$9°$ to $33°$ N / $27°$ to $50°$ E
Geremew Lamessa et al. [34]	"Homogenized earthquake catalog and bvalue mapping for Ethiopia and its adjoining regions"	M_w	1960–2016	$4°$ to $20°$ N / $34°$ to $48°$ E

roughly 27%, 25% and 17%, respectively. The Frequency Magnitude Distributions(FMD) slope (b values) ranges from -0.49 $\pm$0.19 to -1.09 $\pm$0.14 for all source zones, with most zones having values around -0.80, obviously depending on the size and seismicity of the source zone. For the whole of Iraq, the highest regional magnitude m_{max} has been predicted to be 7.87 $\pm$0.86. The purpose of the study is to lay the foundation for more sophisticated methodologies and to pave the way for a probabilistic assessment of the seismic risk of Iraq [36].

An earthquake inventory for the United Arab Emirates region is offered, covering the years 3000 BC to 1 August 2007. The compilation includes conversion of different magnitude scales to M_w if none of the sources provide it; identification of foreshocks and aftershocks using a hybrid method based on the Reasenberg (1985) and Knopoff (2000) window algorithms; and completeness analysis of the homogenized earthquake catalog for various magnitude thresholds. The catalog was created for an area defined as $47°$ E to $66°$ E and $21°$ N to $31°$ N, and it included all occurrences with magnitudes of $4M_w$ or higher. A complete examination of available research on the origins of historical earthquakes (i.e., time, location, depth, and magnitude) has been conducted, as well as systematic re-assessments of the locations and magnitude of instrumental events. It is worth noting the lack of occurrences along the UAE's west coast, which contradicts the likely existence of a primary active fault running along the west coast as seen on Johnson's Tectonic Map of Saudi Arabia and Adjacent Areas (1998) [37].

In this research, the process for creating a catalog of artificially generated earthquakes in northern Iran is presented. The research area includes the northern limit of the central Iranian plateau, which corresponds to the Alborz Mountains. Figure 11 shows line segments that indicate the direction of probable fault ruptures.

In this technique, the attribute information supplied to each line segment can range from the basic azimuth and angle of detachment to other complex geometric metrics that define the entire 3D rupture plane(Figure 11a). This approach can calculate the epicentral distance (Figure 11b) and a fault rupture's closest distance to its surface projection (Figure 11c). These are the most common source-to-site distance definitions found in many ground motion prediction equations. The method and use of Monte Carlo simulation in the assessment of seismic hazards are explored. This approach simulates a wide range of earthquake scenarios while capturing regional seismotectonic properties. The results reveal that the hazard curves are highly sensitive to the length of the simulated earthquake catalogs, especially for long return periods [38].

From 2000 BC to 2009 AD, the seismic database was created for "Central Asia (Kazakhstan, Kyrgyzstan, Tajikistan, Uzbekistan, and Turkmenistan)" as part of the Earthquake Model Central Asia (EMCA) project, the library contains 33,034 earthquakes with MLH magnitudes
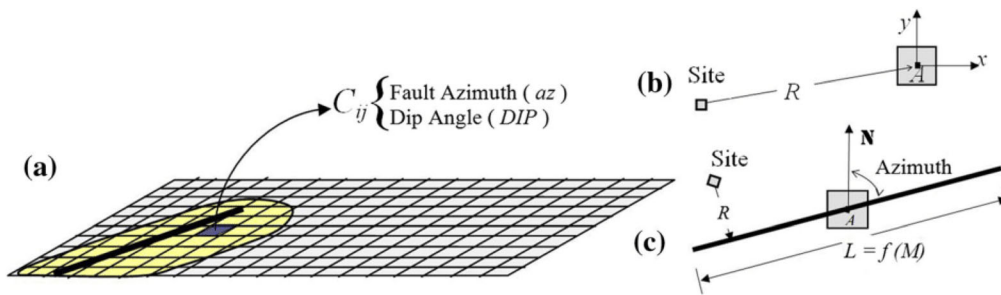
Figure 11. Source system based on cells, **a.** For each cell, defect attribute data is simulated. **b.** Epicentral distance, **c.** proximity to the fault line [38].

ranging from 1.5 to 8.3 on the Richter scale (Surface wave magnitude on horizontal components is a term commonly used in former Soviet Union countries). According to the magnitude of the completeness study, with a regional b value of 0.805 found, the catalog is complete down to magnitude 4 from 1959 and magnitude 7 from 1873. A future study will examine the regression analysis used to assign an MLH value to each entry, as well as the magnitude of the moment M_w [39].

"The International Seismological Center, the Global Centroid Moment Tensor (GCMT), the US Geological Survey, the India Meteorological Department" and published literature were used to compile an earthquake catalog for South Asia spanning the years 1900-2014. By connecting the magnitude categories, a uniform magnitude scale is achieved in the magnitude of the moment $M_{W,GCMT}$. The source spectral features are source dependent and vary across tectonic provinces, including active subduction zones of "the Hindu Kush-Pamir", stable mid-plate areas, and normal-faulting dominated ridge zones. The relationships between $M_{S,ISC}$, $m_{b,ISC}$, $M_{L,ISC}$, $m_{w,USGS}$, and $M_{w,GCMT}$ are shown to be highly consistent with the preceding ones. Braunmiller and Nabelek (2002), on the other hand, found a larger discrepancy of 0.46 units between $M_{w,GCMT}$ and $m_{b,ISC}$ for the investigated region. The associations between $m_{b,ISC}$ and $m_{pv,ISC}$ are identical to those provided by Thingbaijam. We noticed a significant increase in the number of occurrences after 1964, in the data volume, as well as an increase in the number of foreshocks and aftershocks. This is related to improved event detection instrumentation [40].

This article explains how to create and process an updated earthquake inventory for Pakistan. The earthquake database for the region (quadrangle constrained by geographical parameters "40° - 83 ° N and 20° - 40 ° E") in this study contains 36,563 earthquake events that range in magnitude from 4.0 to 8.3 M_W and cover the years 25 AD to 2016. Earthquake occurrences are recorded in "m_b, M_S, M_W, M_L, Modified Mercalli Intensity (MMI), M_N, and M_D magnitude scales" in this collection. At an M_S value of 6.0, in this investigation6.0, in this investigation, the deviation of M_S is observed that matches M_W.is observed that

matches M_W. The correlations are obtained from 762 paired M_S/M_W occurrences in the collection.

$$M_W = 0.58 \times M_S + 2.46 \quad for \quad 3.5 \leq M_S \leq 6.0 \quad (4)$$

$$M_W = 0.94 \times M_S + 0.36 \quad for \quad 6.1 \leq M_S \leq 8.2 \quad (5)$$

At an M_S value of 6.0, in this investigation6.0, in this investigation the deviation of M_S is observed that matches M_W.is observed that matches M_W. Bilinear connections are created and utilised to convert M_S to MW [Eqs. (4) and (5)].

The declustering methods demonstrate the existence of epistemic uncertainty, which must be included in Pakistan's seismic hazard calculations. Using these approaches, the declustered library is then processed to estimate the parameters of the relationship "the Gutenberg and Richter" (1944) for 20 probable seismic sources (deep and shallow) in Pakistan. The western Makran and the Hindu Kush areas have a completion magnitude (M_C) of at least 4.4. The activity rate of shallow seismic sources ranges from 0.376 to 35.809, whereas deep seismic sources have an activity rate ranging from 2.032 to 16.569 [41].

Table 5 shows the comparative analysis of the Asia Catalog. The comparison is made between different magnitudes used in the catalog, the year of the catalog, and the latitude and longitude of the area where the earthquake occurred.

2.5 *Greece Catalog*

An earthquake catalog for Greece from 1900 to 1985 is offered. It builds on previous work from a few years ago. The current edition has more than twice as many events as the previous papers, with 4310 events compared to 1806 events. It also covers 1711 other occurrences that occurred in the region. Furthermore, the inclusion of such a large number of earthquakes, mostly of small to moderate magnitude (M ≤ 5.9) earthquakes, raises issues and decreases the size at which the collection can be considered comprehensive. In both catalogs, the following parameters are recorded for each earthquake: (1) the date, (2) the time of origin, (3) latitude, (4) longitude, (5) focal depth, (6) the

Table 5. Comparative study of Africa Catalog

Author	Title	Magnitude	Year	Lat/Long
David A. Rhoades et al. [35]	"Test of the EEPAS Forecasting Model on the Japan Earthquake Catalogue"	M	1968–2000	$32.3°$ to $44.3°$ N / $131.6°$ to $148.9°$ E
A.S.Ameer et al. [36]	"Probabilistic Seismic Hazard Assessment for Iraq Using Complete Earthquake Catalogue Files"	M_s	1905–2000	$29°$ to $38.5°$ N / $39°$ to $50°$ E
G. Aldama-Bustos et al. [37]	"An earthquake catalogcatalog for the analysis of seismic hazards in the United Arab Emirates"	M_w	3000 BC–2007	$47°$ to $66°$ E / $21°$ to $31°$ N
Mohammad R. Zolfaghari [38]	"Development of a synthetically generated earthquake catalog towards assessment of probabilistic seismic hazard for Tehran"	M_w	400 B.C.–1900	N.A.
Natalya N. Mikhailova et al. [39]	"Central Asia earthquake catalog from ancient time to 2009"	M_L and M_s	2000 BC–2009 AD	$46°$ N / $80°$ E
Sankar Kumar Nath et al. [40]	"A unified earthquake catalog for South Asia covering the period 1900-2014"	M_w, $GCMT$, M_L, M_s and M_D	1900–2014	$3.27°$ to $38.5°$ N to $4.2°$ to $101.24°$ E
Sarfraz Khan et al. [41]	"Updated earthquake catalog for seismic hazard analysis in Pakistan"	M_w	25 AD–2016	$40°$ to $83°$ N / $20°$ $40°$ E

number of reporting stations, and (7) the magnitude of the surface wave. For relocated occurrences (1917–1963), the focal error is estimated to be less than *pm* 10 km for h 50 km and less than ± 15 km for h ≥ 50 km (Makropoulos and Burton 1981). Instead of the number of reporting stations, the relevant reference is supplied covering the years 1900-1963, as well as earthquakes that do not enable relocation. Since 1907, ground-amplitude measurements from the Swedish network have been used to determine the magnitudes of all surface waves in the primary collection. The standard deviation for these magnitudes is around ±0.3 [42].

The seismic frequency textures for Greece as a whole, as well as for the subzones, reveal a long memory; despite this, only the textures for the Hellenic Arc zone ($M_S \geq 5.0$) and Greece as a whole ($M_S \geq 4.0$) approach demonstrable nonrandom patterns. Aside from these, other patterns emerge by chance. In this work, Hurst's approach was used to the creation of a new earthquake database for Greece to uncover some underlying temporal fractal properties for seismicity in Greece. Although both the strain release temporal textures for magnitudes $M_S \geq 5.0$ and $M_S \geq 4.0$ for Greece and its subzones appear to have a long memory or to be Brownian, when evidence from Monte Carlo simulation is presented, they all turn out to be random and memoryless patterns. In other words, these patterns are purely random. Monte Carlo techniques were used to generate time series modeling various physical properties of seismicity, and many simulations were presented to verify that conclusions regarding natural seismicity were highly improbable to have happened by coincidence. The use of this unique approach to characterizing the memory or fractal texture content of seismicity should be regarded as a significant step in the selection of suitable statistical models to estimate earthquake threat [43].

To optimize your capacity to anticipate earthquakes of magnitude 6.0 and more in the period 1966-1980, for magnitudes 4.0 and above, time-invariant, long-range, and short-range forecasting models were fitted to the Greek earthquake database. Predicting the performance of each model was then obtained when the log-likelihood statistic is used, which was applied to the catalog from 1981 to 2002. According to the current assessment of the relative utility of time-invariant, long-range, and short-range forecasting models, the impending occurrence of a significant earthquake is typically signaled by precursory changes in earthquake occurrence patterns in time, location, and magnitude. The current work indicates future research directions for improving long-term and short-term forecasting models. There are two obvious short-term prospects. First, the use of a long-term forecasting model rather than a time-invariant model for the spontaneous component of seismicity may enhance short-term forecasting. Second, long-term forecasting can be improved by taking into account that each projected earthquake is likely to produce aftershocks, some of which may exceed the magnitude

threshold of interest. Finally, the likelihood-based approach used here and elsewhere allows a systematic approach to forecasting improvement through formal testing of proposed model refinements, which can lead to significantly improved forecasting models on a variety of timescales that use not only earthquake catalog data, but also other related geophysical data and modeling in the long run [44].

A homogeneous earthquake catalog is offered that spans Greece and nearby areas from 1900 to 2009, which can be used for credible seismic hazard evaluations. It offers a homogeneous magnitude inventory that includes both the M_s and M_w scales. The expanded collection has 7352 occurrences, which is 70% more than the previously published (1989) version's 4310 events. The examination region is confined, as in earlier editions of the catalogue, to "latitudes 33° N to 42.5° N" and "longitudes 19° E to 29° E north" and south of the 38° N parallel, with $M_s = 4.0$ as the threshold magnitude. For all occurrences since 1900, the magnitude of the moment M_w was calculated. This was done by applying the Eq. (6) connection between M_s and M_w, which was determined using linear regression with 559 directly computed moment magnitudes in the magnitude range of $3.6 \geq M_w \geq 6.8$. Using linear regression, a link was discovered between the amplitude of the surface wave Ms and the magnitude of the moment M_w (Figure 12):

$$M_W = 0.8786M_S + 0.58(R^2 = 0.82, \sigma = \pm 0.26) \quad (6)$$

where R^2 is the quality of fit and σ is the standard deviation.

The 132 final catalog occurrences with $M_w \geq 6.0$, a criterion that corresponds to Greece's most likely yearly maximum. The data sets were treated identically to maintain the high degree of homogeneity and correctness attained in prior released editions of the catalogue [45].

Table 6 shows the comparative analysis of the Greece Catalog. Comparisons are made between different magnitudes used in the catalog, the year of the catalog, and the latitude and longitude of the area where the earthquake occurred.

2.6 *India Catalog*

The usefulness of a newly compiled database of earthquakes that occurred in peninsular India between the years 1849 and 1900 is briefly reviewed in this article. This catalog was compiled using reports from three different newspapers: the Times of India, the Statesman, and the Hindu. Earthquakes of equivalent magnitude have recently occurred in the inventory; earthquakes occurred in "Hyderabad (30 June 1983; magnitude 4.8) and Bangalore (20 March 1985; magnitude 4.5)", confirming its use in estimating the risk of earthquakes. There is an urgent need to scan historical documents in various Indian languages to expand the Indian earthquake database to levels comparable to those found in China and Japan, where data are
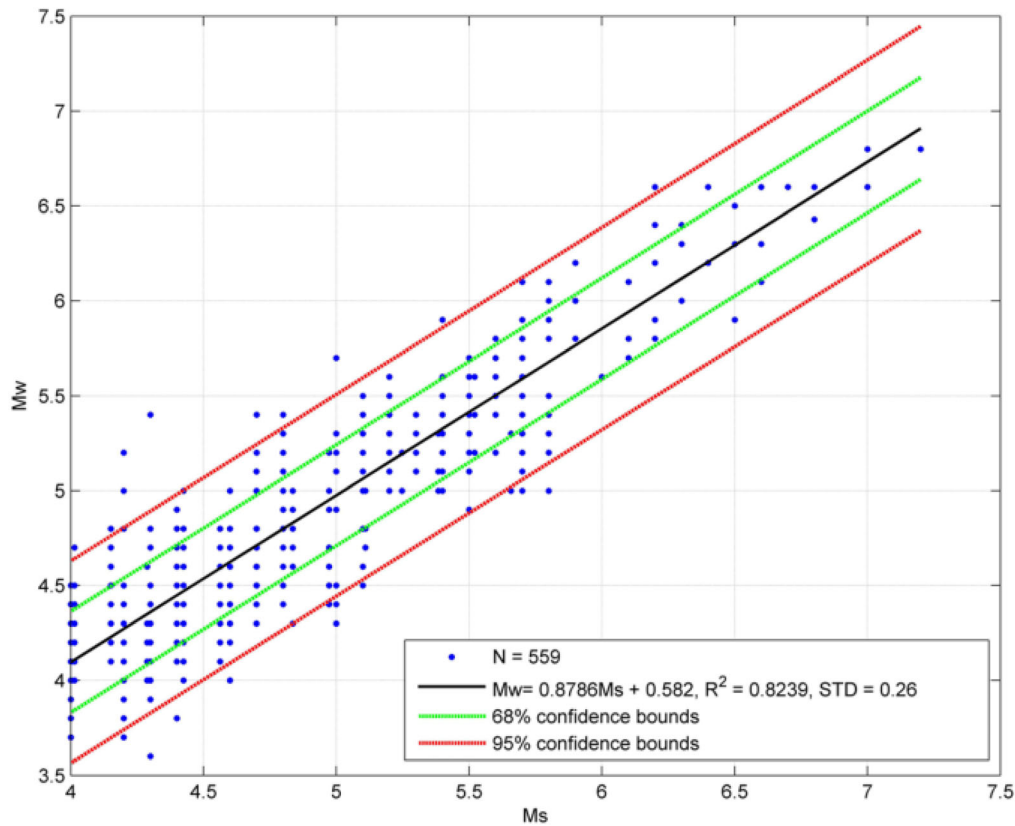
Figure 12. M_w of the moment versus M_w of the Greek surface wave catalog m_s [45].

accessible for 2000 to 3000 years. India Meteorological Department(IMD) is a participant in the IASPEI Historical Seismogram Film Project, which will allow us to use analytic tools (presently available or to be created in the future) to preserve original seismograms at an opportune moment. Over 20,000 records have been microfilmed so far at the Bombay facility designated for the endeavor. The exchange of historical seismograms for big earthquakes will allow us to research seismological problems in the Indian area and other seismic locations throughout the world from both a close and a far-field aspect [46].

For the period 1897-2009, a database of 4,497 earthquake occurrences in northeast India and the surrounding region is gathered for homogeneity with $M_{w,GCMT}$ moment magnitude in the 3-8.7 range. Relationships for the conversion of m_b and M_s magnitudes to $M_{w,GCMT}$ are created for different magnitude ranges using three different approaches, based on occurrence data from 1976 to 2006. Based on 17 occurrences in the range of $5.2 \leq$ magnitude ≤ 6.6, a link between $M_{w,GCMT}$ and $M_{w,NEIC}$ is also discovered. The primary goal of this project is to close the gap in accurate OSR relationships for catalog homogenization in northeast India and the surrounding region. Furthermore, regression correlations between $M_{w,GCMT}$ and $M_{w,NEIC}$ are found, demonstrating that M_w estimations from GCMT and

NEIC may be viewed as equal. Since $\sqrt{\eta} \leq 0.7$, we choose the ISR relation to convert m_b to $M_{w,GCMT}$. Because data for smaller body wave magnitudes, such as $m_b \leq 4.6$, is rare, no regression relationship is tried. As demonstrated by fewer uncertainties in the regression parameters, this study shows that the Orthogonal Standard Regression (OSR) and inverted standard regression (ISR) conversion relationships for the analyzed region have improved. A homogenized catalog based on these relations should result in fewer uncertainties in unified moment magnitude estimations, which are critical inputs for the estimation of seismic hazards and other seismological investigations [47].

Northeast India is one of the most seismically active regions on the planet. The event data utilized in this study were mostly derived from the worldwide ISC, NEIC, and GCMT databases for the years 1897 to 2010. Data from the India Meteorological Department Bulletins and a historical seismicity inventory are also used. An Orthogonal Standard Regression (OSR) link was also discovered for scaling intensity estimations to $M_{w,NEIC}$ using 126 global intensity occurrences with intensity VI or higher from 1975 to 2010. The northeast (NE) India region is one of the most seismically prone locations in the world, characterized by the geographical coordinates 20° - 30° N latitude and 87° - 98° E longitude. Four catalog eras have been considered: 1897-

Table 6. Comparative study of Greece Catalog.

Author	Title	Magnitude	Year	Lat/Long
K. C. Makropoulos et al. [42]	"A revised and extended earthquake catalog for Greece since 1900"	M_s	1900–1985	33° to 42.5° N / 19° to 29° E
Yebang Xu et al. [43]	"Time-varying seismicity in Greece: Hurst's analysis and Monte Carlo simulation applied to a new earthquake catalog for Greece"	M_s	1964–1999	33° to 43° N / 18° to 31° E
R.Console et al. [44]	"Comparative performance of time-invariant, long-range and short-range forecasting models on the earthquake catalogue of Greece"	M	1966–2002	33° to 42.5° N / 18° to 30° E
K. Makropoulos et al. [45]	"An updated and extended earthquake catalog for Greece and adjacent areas since 1900"	M_s and M_w	1900–2009	33° to 42.5° N / 19° to 29° E

1963, 1964-1990, 1964-2000, and 1964-2010. Surface wave magnitude conversion formulae for the ranges $4.1 \leq M_{s,ISC} \leq 6.9$ and $4.8 \leq M_{s,NEIC} \leq 6.2$ have been created, using data from 98 and 59 occurrences from 1978 to 2006. The Uhrhammer (1986) approach was used to decluster the homogenized catalog for the period 1897-2010, resulting in a decrease of 905 events (24.4%). Catalog data for the years 1897-2010 show that there have been no earthquakes of magnitude ≥ 7.0 in zones I, VI, or IX. Because zone IX is located between zones IV and VII, both of which have experienced substantial earthquakes, the risk of a large earthquake occurring in this region appears to be low compared to other zones [48].

Earthquake data for the Northeast area of India from the International Seismological Center and the Global Centroid Moment Tensor databases, chronologically, from 1 January 1900 to 31 April 2016. With a 90% confidence level, the magnitude of completeness for space and time has been realized. The seismicity parameters M_C, the value of a, and the value of b are calculated to be 4.6, 7.50, and 0.95 (± 0.023), respectively. Furthermore, the Uhrhammer (1986) approach was used to decluster the homogenized catalog in this region. The expected value of M_C is 4.6 from the FMD of earthquakes based on this declustered library, as illustrated in Figure 13.

The completeness for the time was also examined using a simple visual cumulative approach, and since 1993, 1986, 1963, and 1902, the magnitudes $M_W \geq 3.0$, $M_W \geq 4.0$, $M_W \geq 5.0$, and $M_W \geq 6.0$ are complete and stable, respectively. The random distribution of occurrences above and below the average number of incidences per hour of 153 adds to this. As a consequence, the improved and homogenized earthquake catalog created in M_W can significantly reflect the true values of seismicity parameters to determine seismicity hazard levels in this earthquake-prone region [49].

Table 7 shows the comparative analysis of the India catalog. Comparisons are made between different magnitudes used in the catalog, the year of the catalog, and the latitude and longitude of the area where the earthquake occurred.

2.7 Global Catalog

Our database provides information on the location, amplitude, seismic moment, and focal mechanisms of more than 1300 previously and instrumentally reported M (moment magnitude) ≥ 4.5 crustal earthquakes. Based on its location, each tectonic event is assigned to one of five groups: (i) internal gaps/taphrogens, (ii) rifted continental edges, (iii) non-rifted crust, (iv) probable interior rifts, and (v) possibly rifted margins. We observe that around (i) 27% of all occurrences are classified as inner rifts. (ii) 25% as rifted continental borders; (iii) 36% as nonrifted crust; (iv) 12% and (v) uncertain. When only large earthquakes (M ≤ 6.0)

are evaluated, there is no significant change in distribution. However, the greatest events ($M \geq 7.0$) have predominantly occurred within rifts (50*percent*) and along continental margins (43*percent*). Intraplate seismicity is not uniformly distributed. After excluding non-tectonic earthquakes, to reevaluate the relationship of earthquakes with ancient rifts on a global scale, 1221 tectonic events were used for statistical analysis. Interior rifts/taphrogens accounted for 27% of the earthquakes, rifted continental edges accounted for 25%, non-rifted crust accounted for 36%, and the other 12% were unknown. When only the bigger events ($M \geq 6.0$) are studied, the percentages remain fairly similar, although inner rifts/taphrogens (50%) and rifted continental margins (43%) prevail for the largest events ($M \geq 7$, $N = 14$), outer rifts/taphrogens (43*percent*) dominate. To summarise, while there have been several earthquakes within the rifted crust, the potential for seismicity within rifts should not be underestimated [50].

The Global Instrumental Earthquake Catalog (1900 - 2009) of the International Seismological Center-Global Earthquake Model (ISC - GEM) is the result of a concentrated effort to greatly extend and improve current worldwide libraries to suit the demands of various user groups that analyze and model seismic hazards and risks. 110 years of earthquake hypocenters and uncertainty, computed with the original arrival time data and the same methodology and velocity model. Each event in the catalog has a magnitude with uncertainty on the scale M_w ascribed to it. In all other cases (the vast majority before 1976), proxy M_w estimations were used, which were based on newly discovered empirical linkages with M_S and m_b. As part of this study, all M_S and m_b were recalculated utilizing the original amplitude and period data from high-quality long-term locations. On a worldwide scale, we see a shift in completeness from M_w 5.6 before 1964 to M_w 6.4 thereafter. This is, of course, a direct result of the change in cutoff magnitude associated with the start of ISC operations and the following large increase in parametric data availability. Seismicity rates for large earthquakes ($M_w \geq 7.5$-7.6) are best estimated over time [51].

The Global History Earthquake Archive (GHEA) provides an in-depth description of the world's position in big earthquake history seismology. The Global Historical Earthquake Catalog (GHEC v1.0) was created from GHEA, a global inventory of earthquakes with magnitudes of M_w 7 and greater for the period 1000-1903.

GHEC v1.0 contains 825 earthquakes (Figure 14), the parameters of which were derived from 87 sources, of which 8 were only evaluated for magnitude and 4 for epicenters. Seventy different sources are used to calculate the magnitudes and locations of 715 earthquakes $M \geq 7$. When it is stated in more than one scale in the original catalog, the hierarchy of (i) M_w, (ii) M_s, and (iii) additional types were used. Aside from saturation issues, scales with magnitudes ranging from 6.5 to 8 tend to converge. Given the high magnitude threshold of the catalog, the magnitudes
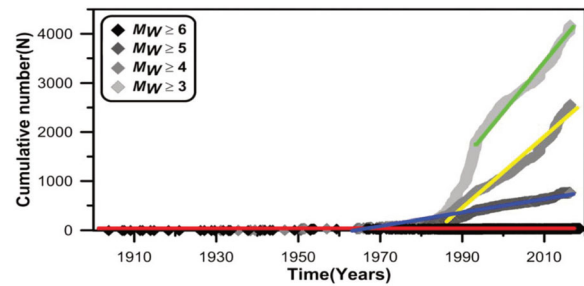

Figure 13. Graph depicting the examination of the earthquake's completeness period by charting time (years) and cumulative number of occurrences for a range of earthquake magnitudes [49].

represented in M_s can be considered similar to the magnitudes reported in M_w [52].

The process of recalculating and combining the magnitudes currently included in the final ISC-GEM Reference Global Instrumental Earthquake Catalog is described in this article (1900-2009). We have made every effort to apply consistent magnitude determination methodologies throughout the catalog. We analyzed an unusual amount of data, in particular from M_S through the end of 1970, and obtained many thousands of previously inaccessible station magnitudes. The recalculated M_S and m_b provided a good foundation for developing new moment magnitude M_W conversion formulae. Throughout the 110 years covered by the ISC-GEM catalog, the magnitude completeness is not uniform. As a result, without proper temporal window selection, the seismicity rate estimation can be greatly influenced. Although the completeness for the early instrumental period varied from 7.5 to 6.2, the ISC-GEM library appears to be comprehensive up to M_W 5.6 beginning in 1964. More effort and resources would be necessary to spread the scale of completeness equally across the entire catalog length. Throughout the 110 years covered by the ISC-GEM catalog, the magnitude completeness is not uniform. The time-M_c distribution reflects this, and without careful time frame selection, seismicity rate estimation may be greatly influenced. To homogenize the completeness of the magnitude across the length of the catalog, a tremendous amount of labor and money would be required [53].

The results of a two-year experiment funded by the ISC-GEM Worldwide Library of the Global Earthquake Model (GEM) Foundation contain approximately 19,000 moderate to large earthquakes that were instrumentally documented throughout 110 years of seismicity. Using a two-tier strategy, we moved all events in the catalog. Between 1904 and 1970, approximately one million seismic P and S wave arrival time data were collected and added to the ISC database, either from original station bulletins in the ISC collection or from digitized copies of the "International Seismological Summary" (ISS) bulletin, to aid in the relocation effort. We show that the ISC-GEM catalog gives an enhanced perspective of the Earth's seismicity during

Table 7. Comparative study of India Catalog.

Author	Title	Magnitude	Year	Lat/Long
H.N. Srivastava et al. [46]	"Historical seismicity and earthquake catalogues for the Indian region"	M	1849–1900	5° to 28° N / 67.5° to 90° E
Ranjit Das et al. [47]	"Homogenization of Earthquake Catalog for Northeast India and Adjoining Region"	M_w, M_s and m_b	1897–2009	20° to 32° N / 87° to 100° E
Ranjit Das et al. [48]	"Temporal and spatial variations in the magnitude of completeness for homogenized moment magnitude catalog for northeast India"	M_w	1975–2010	20° to 30° N / 87° to 98° E
Auchitya Kumar Pandey et al. [49]	"Homogeneous earthquake catalog for Northeast region of India using robust statistical approaches"	M_s, M_L, m_b & M_w	1900–2016	21° to 30° N / 87° to 98° E

the last 110 years, with significant advances in predictions of focal depth in subduction zones and other seismically active locations. There were insufficient amplitude observations for a lot of occurrences without a direct measure of M_W, it is impossible to determine m_b or M_S. Moreover, because body wave magnitudes were first recorded routinely around the latter half of the twentieth century, many early deep events have no estimated magnitude and therefore cannot be included in the main ISC-GEM database. We felt it was important to create a supplementary catalog to the ISC-GEM database that contains 858 large earthquakes with no magnitude estimates, as well as 45 events with less reliable locations [54].

A complete overview of the ISC-GEM Global Instrumental Earthquake Catalog (1900-2009). The two-and-a-half-year inquiry provided a collection of over 20,000 major earthquakes spanning 110 years, with hypocentres and uncertainties computed using the same approach and velocity model. The magnitude and uncertainties of each earthquake were calculated using existing seismic moment estimates or unique empirical links between M_W, M_S, and m_b. We explain why such a catalog is necessary for a thorough evaluation of seismic risk on a global and regional scale. We also discuss the catalog's possible applications in a variety of other Earth sciences fields. We examine the catalog's availability and future development goals. We would like to remind catalog users that the M_W type is differentiated in the catalog by M_W values computed directly (d) from seismic moments and M_W proxy (p) values computed using regressions from M_S and m_b. This project has several significant adverse effects. Large amounts of previously inaccessible fundamental parametric data have been digitized and made available to users. As a result of this strategy, several previously inaccessible M_S and m_b are now available. A contribution was also made to the expansion of the ISC Event Bibliography [55].

The creation of a magnitude-homogenized inventory is a critical element in seismic hazard assessment. In addition to its verified global bulletins, the International Seismological Center (ISC) database offers the most complete collection of local bulletin recordings. The first is an important application in Sub-Saharan Africa that compares the geographical coverage and magnitude scales of several local recording networks to global magnitude scales. The technologies are used on a worldwide scale in the second application to create an expanded global earthquake database with uniform magnitudes. Several high-quality earthquake datasets, including ISC-GEM and ISC-reviewed bulletins, have been harmonized by moment magnitude to provide a catalog of about 562,840 occurrences. Many hazard models are aware of the homogenization process, but the specifics of implementation are rarely discussed. Future improvements will include direct support for catalogs in various formats as
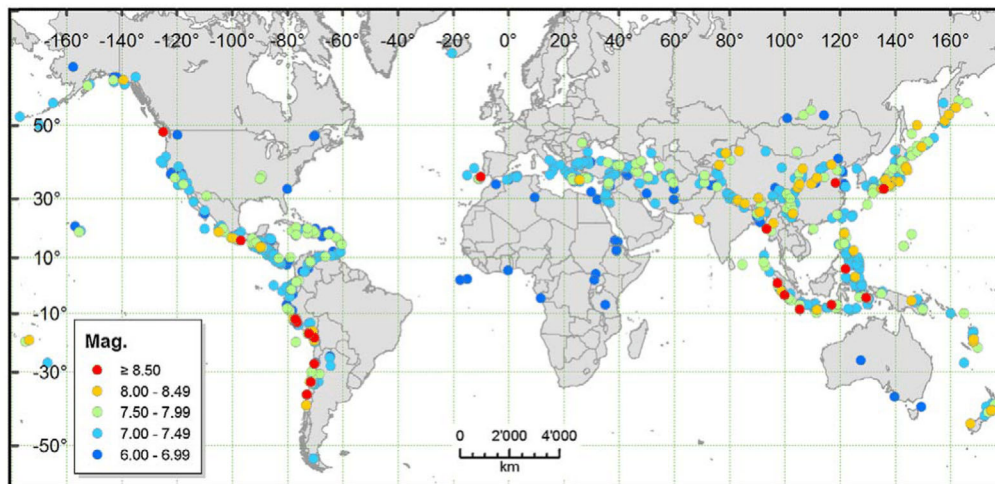
Figure 14. The 825 earthquakes in GHEC v1.0 are classified according to their magnitude [52].

well as a large increase in the capacity to analyze moment tensor data. Some functionality to create moment tensor databases and connect them to the general catalog database is already in place, but additional tools to compile and process databases of moment tensor solutions could be useful in incorporating seismotectonic interpretation into the data assembly process [56].

Global seismicity models provide scientific hypotheses on the frequency, location, and magnitude of future earthquakes throughout the planet. In the development and testing of two revised global earthquake models to provide a risk assessment, the mean shallow seismicity values (d $\leq$ 70 km) are used. The "Subduction Megathrust Earthquake Rate Forecast" (SMERF2) is a subduction zone earthquake rate model restricted by geodetic strain measurements and earthquake catalog data, which is used in these approaches, known as "the Tectonic Earthquake Activity Model" (TEAM) and "the World Hybrid Earthquake Estimates based on likelihood scores" (WHEEL). As a consequence, among all participant earthquake forecasts, During the pseudoprospective test period, GEAR1 and WHEEL are the most informative seismicity predictions, with the greatest information gain scores (see Fig. 15).

The TEAM and WHEEL calibration periods are January 1, 1977, through December 31, 2013. As a consequence, we utilized m $\geq$ 5.95 earthquakes reported between 2014 and 2019 to assess the forecasting capacities of several earthquake models and statistically compare their performance to the global earthquake activity rate model (GEAR1). The comparative T-test results reveal that the Kagan Jackson Smo-othed Seismicity (KJSS) exceeds the prediction skills of TEAM and SHIFT GSRM2 throughout a 6-year pseudo prospective assessment period. Interestingly, despite the existence of intermediate-size tectonic events such as 2016 m_w = 7.9 Papua Neuve Guinea, 2016 m_w = 7.8 Solomon Islands, and 2017 m_w = 8.2 Mexico earthquakes, these
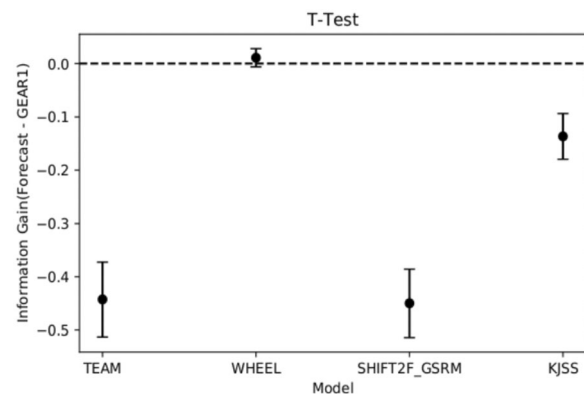

Figure 15. Comparisons of T-tests of rival global seismicity models for the pseudo-prospective assessment period 2014-2019. Although they are not presented, the findings of the W-test corroborate all the results of the T-test [57].

estimates overestimate global earthquake activity during the time frame 1 January 2016-31 December 2017 [57].

Table 8 shows the comparative analysis of the Global Catalog. Comparisons are man-made Comparisons are made between different magnitudes used in the catalog, the year of the catalog, and the latitude and longitude of the area where the earthquake occurred.

3. Gaps in Literature

The absence of standards in the current catalog highlighted the need for a simpler and more up-to-date catalog to aid in earthquake-related risk and hazard assessments. The primary purpose of PSHA is to estimate the rate at which the defined limits of ground motion will be exceeded at a location in the event of future earthquakes. This

characteristic of PSHA allows us to examine structural demands within a stochastic framework, which may then be linked to seismic susceptibility and risk, both of which are critical components of the assessment of seismic loss and decision procedures. The BSHAP earthquake catalog used in this study is consistent with well-established European and global catalogs, and it will serve as a strong foundation for future seismic hazard estimations in the Balkan region and its neighboring territories.

For more advanced regression models with distinct errors, the GOR1 method is preferred [58, 59]. The data that has been filtered, cleaned, and rectified will be beneficial in the development of future seismicity models, as well as the assessment of seismic hazards and risks. Temporary deployments and theoretical modeling have revealed that ocean-bottom seismometers might significantly improve offshore monitoring. These data sets should help and improve future earthquake investigations. There are several earthquake catalogs or data sets available for Turkey and the surrounding region, but these are very limited and do not meet the standards for earthquake risk assessment and risk assessment.

4. Future Direction

Catalogs provide important basic data for future research. Using the revised earthquake catalog and the integrated intermediate output earthquake database from this work, we expect to make a significant contribution to future earthquake-related research, particularly seismic risk assessment and risk assessment studies in Turkey and its neighboring areas. These aseismic patches are particularly significant because they may represent creeping segments or frozen fault asperities, and hence the nucleation point of future
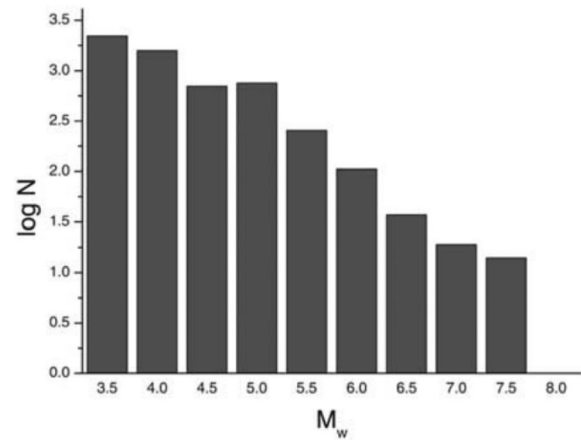

Figure 16. The magnitude-frequency histogram of earthquakes in the catalog. Events in the Atlantic Ocean and Iceland (AOI) polygons have been eliminated. Although the Catalogue's magnitude requirement is $M_w = 3.50$, occurrences with magnitudes as low as $M_w = 3.25$ have been utilised for the lowest magnitude [20].

ruptures. We believe that the BSHAP earthquake catalog presented in this study is congruent with well-established European and worldwide catalogs and that it will provide a solid platform for future seismic hazard calculations in the Balkan Region and its environs. The adoption of updated velocity models is projected to result in even greater gains.

During the international seismic hazard analyses of the Sinop Nuclear Power Plant, which is scheduled for construction in the far north of Turkey for future research, it became evident that Turkey needs a comprehensive homogenized seismic inventory. Future Databank updates should contain not only the extension of the historical span of the local catalogs but also data from other specialized research. Because catalog work is a never-ending effort,

Table 8. Comparative study of Global Catalog.

Author	Title	Magnitude	Year	Lat/Long
Dmitry A. Storchak et al. [51]	"Public Release of the ISC-GEM Global Instrumental Earthquake Catalog (1900-2009)"	M_w	1900–2009	Different Ranges
Paola Albini et al. [52]	"The Global Earthquake History"	M_w	1000–1903	Different Ranges
Domenico Di Giacomo et al. [53]	"ISC-GEM: Global Instrumental Earthquake Catalog (1900-2009), III. Re-computed M_S and m_b, proxy M_W, final magnitude composition and completeness assessment"	M_s, m_b, M_w	1905–2009	Different Ranges
Bondár et al. [54]	"ISC-GEM: Global Instrumental Earthquake Catalogue (1900-2009), II. Location and Seismicity Patterns"	M_s, m_b and M_w	1900–2009	Different Ranges

future research may reveal how this catalog might be enhanced and refined. The importance of showing the geographical and temporal heterogeneities of earthquake catalogs to enable future evaluation of the seismicity of the region. The Catalog, according to the authors, will be useful for a wide range of applications in seismology and seismic hazard. This is important preliminary research for any future earthquake forecasting or regional seismic hazard assessment investigations.

5. Conclusion

It is well known that the fault system is capable of producing severe earthquakes, with six big events ($M \geq 6.5$) occurring between 1939 and 1957 in Turkey. A more comprehensive earthquake inventory has been created to serve as a resource for the UDSEP-2023's continuing projects, Turkey's Seismotectonic Map and Turkey's Seismic Hazard Map. The homogeneous and declustered collection produced of 6573 occurrences serves as a basis for a credible contribution to seismic studies on risk assessment for Turkey and its neighbors. Figure 16 shows a histogram of the magnitude distribution of all occurrences, except for the polygon Atlantic Ocean and Iceland for the period 1300-1993.

Earthquake Catalog of Switzerland (ECOS) is distinguished by a consistent evaluation of earthquake parameters, comprising the identification of error limits for all source parameters and a standard magnitude M_W for all occurrences. This database contains the parameters of historical earthquakes as well as the focal mechanism parameters of 108 damaging earthquakes.

The primary goal of the European-Mediterranean Earthquake Catalog (EMEC) catalog is to provide a resource for seismic hazard computation, however, it may also be used for a variety of seismicity research. For the first time in this database, precise maps of M_c are calculated throughout many periods at each studied location. The entire active rift zone of the north-south has a relatively low completeness magnitude M_c in the range of 0.5 to 1.0, demonstrating the capacity of the Icelandic network to detect minor earthquakes. This study also shows how earthquake location uncertainty influences the Spatio-temporal magnitude of completeness analyzes. In areas with high station coverage, the BMC standard deviation could be as low as 0.1.

References

[1] Lubbers N, Bolton D C, Mohd-Yusof J, Marone C, Barros K and Johnson P A 2018 Earthquake catalog-based machine learning identification of laboratory fault states and the effects of magnitude of completeness. *Geophysical Research Letters* 45(24): 13–269

[2] Schoenball M and Ellsworth W L 2017 Waveform-relocated earthquake catalog for Oklahoma and southern Kansas illuminates the regional fault network. *Seismological Research Letters* 88(5): 1252–1258

[3] White M C A, Ben-Zion Y and Vernon F L 2019 A detailed earthquake catalog for the San Jacinto fault-zone region in Southern California. *Journal of Geophysical Research: Solid Earth* 124(7): 6908–6930

[4] Onur T, Gök R, Abdulnaby W, Mahdi H, Numan N M S, Al-Shukri H and Abd N A 2017 A comprehensive earthquake catalog for Iraq in terms of moment magnitude. *Seismological Research Letters* 88(3): 798–811

[5] Aiken C and Obara K 2021. Data-Driven Clustering Reveals More Than 900 Small Magnitude Slow Earthquakes and Their Characteristics. *Geophysical Research Letters*, 48(11), e2020GL091764

[6] Tamaribuchi K, Yagi Y, Enescu B and Hirano S 2018 Characteristics of foreshock activity inferred from the JMA earthquake catalog. *Earth, Planets and Space* 70(1): 1–13

[7] Deniz A and Yücemen M S 2008. Processing earthquake catalog data for seismic hazard analysis. *8th International Congress on Advances in Civil Engineering*, Kuzey Kıbrıs

[8] Badawy A, Gamal M, Farid W and Soliman M S 2019 Decontamination of earthquake catalog from quarry blast events in northern Egypt. *Journal of Seismology* 23(6): 1357–1372

[9] Kano M, Aso N, Matsuzawa T, Ide S, Annoura S and Arai R 2018 Development of a slow earthquake database. *Seismological Research Letters* 89(4): 1566–1575

[10] Igarashi T 2020 Catalog of small repeating earthquakes for the Japanese Islands. *Earth, Planets and Space* 72: 1–8

[11] Alsan E, Tezuçan L and Båth M 1976 An earthquake catalogue for Turkey for the interval 1913–1970. *Tectonophysics* 31(1–2): T13–T19

[12] Tan O, Tapirdamaz M C and Yörük A 2008 The earthquake catalogues for Turkey. *Turkish Journal of Earth Sciences* 17(2): 405–418

[13] Kadirioglu F T, Kartal R F, Kılıç T, Kalafat D, Duman T Y, Ozalp S and Emre O 2014. An improved earthquake catalogue (m $\geq$ 4.0) for turkey and near surrounding (1900–2012). *Proceedings of 2nd European Conference on Earthquake Engineering and Seismology*, İstanbul Aug, 25-29

[14] Kadirioglu F T, Kartal R F, Kilic T, Kalafat D, Duman T Y, Azak T E and Emre O 2018. An improved earthquake catalogue (M $\geq$ 4.0) for Turkey and its near vicinity (1900–2012). *Bulletin of Earthquake Engineering*, 16(8), 3317-3338

[15] Kadirioglu F T and Kartal R F 2016 The new empirical magnitude conversion relations using an improved earthquake catalogue for Turkey and its near vicinity (1900–2012). *Turkish Journal of Earth Sciences* 25(4): 300–310

[16] Azak T E, Kalafat D, Şeşetyan K and Demircioğlu M B 2018 Effects of seismic declustering on seismic hazard assessment: a sensitivity study using the Turkish earthquake catalogue. *Bulletin of Earthquake Engineering* 16(8): 3339–3366

[17] Wollin C, Bohnhoff M, Martínez-Garzón P, Küperkoch L and Raub C 2018 A unified earthquake catalogue for the Sea of Marmara Region, Turkey, based on automatized phase picking and travel-time inversion: Seismotectonic implications. *Tectonophysics* 747: 416–444

[18] Tan O 2021 A homogeneous earthquake catalogue for Turkey. *Natural Hazards and Earth System Sciences* 21(7): 2059–2073

[19] Herak M, Herak D and Markušić S 1996 Revision of the earthquake catalogue and seismicity of Croatia, 1908–1992. *Terra Nova* 8(1): 86–94

[20] Grünthal G and Wahlström R 2003 An M w based earthquake catalogue for central, northern and northwestern Europe using a hierarchy of magnitude conversions. *Journal of Seismology* 7(4): 507–531

[21] Fäh D 2003 Earthquake Catalogue Of Switzerland (ECOS) And The Related Macroseismic Database''. Eclogae geol. Helv, Citeseer

[22] Stromeyer D, Grünthal G and Wahlström R 2004 Chi-square regression for seismic strength parameter relations, and their uncertainties, with applications to an M w based earthquake catalogue for central, northern and northwestern Europe. *Journal of Seismology* 8(1): 143–153

[23] Grünthal G, Stromeyer D and Wahlström R 2009 Harmonization check of M w within the central, northern, and northwestern European earthquake catalogue (CENEC). *Journal of Seismology* 13(4): 613–632

[24] Grünthal G and Wahlström R 2012 The European-Mediterranean earthquake catalogue (EMEC) for the last millennium. *Journal of Seismology* 16(3): 535–570

[25] Panzera F, Zechar J D, Vogfjörd K S and Eberhard D A J 2016 A revised earthquake catalogue for South Iceland. *Pure and Applied Geophysics* 173(1): 97–116

[26] Gonzalez A 2017 The Spanish national earthquake catalogue: evolution, precision and completeness. *Journal of Seismology* 21(3): 435–471

[27] Panzera F, Mignan A and Vogfjoro K S 2017 Spatiotemporal evolution of the completeness magnitude of the Icelandic earthquake catalogue from 1991 to 2013. *Journal of Seismology* 21(4): 615–630

[28] Manchuel K, Traversa P, Baumont D, Cara M, Nayman E and Durouchoux C 2018 The French seismic CATalogue (FCAT-17). *Bulletin of Earthquake Engineering* 16(6): 2227–2251

[29] Radulian M, Bălă A, Ardeleanu L, Toma-Dănilă D, Petrescu L and Popescu E 2019 Revised catalogue of earthquake mechanisms for the events occurred in Romania until the end of twentieth century: REFMC. *Acta Geodaetica et Geophysica* 54(1): 3–18

[30] Lolli B, Randazzo D, Vannucci G and Gasperini P 2020 The HOmogenized instRUmental Seismic catalog (HORUS) of Italy from 1960 to present. *Seismological Society of America* 91(6): 3208–3222

[31] Hussein H M, Abou Elenean K M, Marzouk I A, Peresan A, Korrat I M, El-Nader E A and El-Gabry M N 2008 Integration and magnitude homogenization of the Egyptian earthquake catalogue. *Natural Hazards* 47(3): 525–546

[32] Amponsah P, Leydecker G and Muff R 2012 Earthquake catalogue of Ghana for the time period 1615–2003 with special reference to the tectono-structural evolution of southeast Ghana. *Journal of African Earth Sciences* 75: 1–13

[33] Babiker N, Mula A H G and Others, 2015 A unified Mw-based earthquake catalogue and seismic source zones for the Red Sea region. *Journal of African Earth Sciences* 109: 168–176

[34] Lamessa G, Mammo T and Raghuvanshi T K 2019 Homogenized earthquake catalog and b-value mapping for Ethiopia and its adjoining regions. *Geoenvironmental Disasters* 6(1): 1–24

[35] Rhoades D A and Evison F F 2005 Test of the EEPAS forecasting model on the Japan earthquake catalogue. *Pure and Applied Geophysics* 162(6): 1271–1290

[36] Ameer A S, Sharma M L, Wason H R and Alsinawi S A 2005 Probabilistic seismic hazard assessment for Iraq using complete earthquake catalogue files. *Pure and Applied Geophysics* 162(5): 951–966

[37] Aldama-Bustos G, Bommer J J, Fenton C H and Stafford P J 2009 Probabilistic seismic hazard analysis for rock sites in the cities of Abu Dhabi, Dubai and Ra's Al Khaymah. *United Arab Emirates. Georisk* 3(1): 1–29

[38] Zolfaghari M R 2015 Development of a synthetically generated earthquake catalogue towards assessment of probabilistic seismic hazard for Tehran. *Natural Hazards* 76(1): 497–514

[39] Mikhailova N N, Mukambayev A S, Aristova I, Kulikova G, Ullah S, Pilz M and Others 2015. Central Asia earthquake catalogue from ancient time to 2009. *Annals of Geophysics*, 58(1)

[40] Nath S K, Mandal S, Adhikari M D and Maiti S K 2017 A unified earthquake catalogue for South Asia covering the period 1900–2014. *Natural Hazards* 85(3): 1787–1810

[41] Khan S, Waseem M, Khan M A and Ahmed W 2018 Updated earthquake catalogue for seismic hazard analysis in Pakistan. *Journal of Seismology* 22(4): 841–861

[42] Makropoulos K C, Drakopoulos J K and Latousakis J B 1989 A revised and extended earthquake catalogue for Greece since 1900. *Geophysical Journal International* 98(2): 391–394

[43] Xu Y and Burton P W 2006 Time varying seismicity in Greece: Hurst's analysis and Monte Carlo simulation applied to a new earthquake catalogue for Greece. *Tectonophysics* 423(1–4): 125–136

[44] Console R, Rhoades D A, Murru M, Evison, F F, Papadimitriou E E and Karakostas V G 2006. Comparative performance of time-invariant, long-range and short-range forecasting models on the earthquake catalogue of Greece. *Journal of Geophysical Research: Solid Earth*, 111(B9)

[45] Makropoulos K, Kaviris G and Kouskouna V 2012 An updated and extended earthquake catalogue for Greece and adjacent areas since 1900. *Natural Hazards and Earth System Sciences* 12(5): 1425–1430

[46] Srivastava H N and Das S K 1988. Historical seismicity and earthquake catalogues for the Indian region. *Symposium on Historical Seismograms and Earthquakes*, 335-348

[47] Das R, Wason H R and Sharma M L 2012 Homogenization of earthquake catalog for northeast India and adjoining region. *Pure and Applied Geophysics* 169(4): 725–731

[48] Das R, Wason H R and Sharma M L 2012 Temporal and spatial variations in the magnitude of completeness for homogenized moment magnitude catalog for northeast India. *Journal of Earth System Science* 121(1): 19–28

[49] Pandey A K, Chingtham P and Roy P N S 2017 Homogeneous earthquake catalogue for Northeast region of India using robust statistical approaches. *Geomatics, Natural Hazards and Risk* 8(2): 1477–1491

[50] Schulte S M and Mooney W D 2005 An updated global earthquake catalogue for stable continental regions: reassessing the correlation with ancient rifts. *Geophysical Journal International* 161(3): 707–721

[51] Storchak D A, Di Giacomo D, Bondár I, Engdahl E R, Harris J, Lee W H K and Bormann P 2013 Public release of the ISC-GEM global instrumental earthquake catalogue (1900–2009). *Seismological Research Letters* 84(5): 810–815

[52] Albini P, Musson R M W, Rovida A, Locati M, Gomez Capera A A and Viganò D 2014 The global earthquake history. *Earthquake Spectra* 30(2): 607–624

[53] Storchak D A, Di Giacomo D, Engdahl E R, Harris J, Bondár I, Lee W H K and Villaseñor A 2015 The ISC-GEM global instrumental earthquake catalogue (1900–2009): introduction. *Physics of the Earth and Planetary Interiors* 239: 48–63

[54] Bondár I, Engdahl E R, Villaseñor A, Harris J and Storchak D 2015 ISC-GEM: Global instrumental earthquake catalogue (1900–2009), II. Location and seismicity patterns. *Physics of the Earth and Planetary Interiors* 239: 2–13

[55] Di Giacomo D, Bondár I, Storchak D A, Engdahl E R, Bormann P and Harris J 2015 ISC-GEM: Global Instrumental Earthquake Catalogue (1900–2009), III. Re-computed MS and mb, proxy MW, final magnitude composition and completeness assessment. *Physics of the Earth and Planetary Interiors* 239: 33–47

[56] Weatherill G A, Pagani M and Garcia J 2016 Exploring earthquake databases for the creation of magnitude-homogeneous catalogues: tools for application on a regional and global scale. *Geophysical Journal International* 206(3): 1652–1676

[57] Bayona J A, Savran W, Strader A, Hainzl S, Cotton F and Schorlemmer D 2021 Two global ensemble seismicity models obtained from the combination of interseismic strain measurements and earthquake-catalogue information. *Geophysical Journal International* 224(3): 1945–1955

[58] Das, Ranjit, M.L.Sharma H.R.Wason, Deepankar Chodhury, Gabriel Gonzalez 2019 A seismic moment magnitude scale, Bulletin of Seismological Society of America, 109 (4): 1542-1555, 2019., ISSN NOO: 1943-3573 (print) 0037-1106 (web)

[59] Wason H R, Das R, M L Sharma 2012 Magnitude Conversion Problem Using General Orthogonal Regression. Geophysical Journal International, 190(2), 2012, 1091–1096.